Reviewer Comments (in black**), my response (**in blue**) and revised manuscript passages** (in dark orange**)**

Anonymous Referee #1

General Comments

This manuscript presents a highly detailed study of the cooling and heating effects of alpine rocks in a laboratory and field setting. The author should be commended for capturing this type of data set as it is clear that it has the ability to inform on several key attributes of the geomorphological behaviour of high altitude rock walls. The author makes several interesting points and clearly has collected a significant data set to stand behind some important interpretations. The confirmation of hysteretic thermally generated fracture deformation is a very good contribution, as is the observation that the thermal expansion coefficients are different between cooling and warming. In addition, the observations that snow cover (and lack thereof from future climate change) will affect the cyclic thermal effect at different altitudes is an important result in itself, especially since it is clearly shown by the field data. However, overall, I found the structure and presentation of the manuscript requiring significant revision.

At the outset, the Abstract should summarize the main findings of the research. I found these difficult to identify. The Abstract discusses rock fracture, altitudinal dependence, and climate change, but also presents results on shear plane controls, ice segregation effects, and snow cover. Whereas these latter three items are all part of the overall arching theme of rock fracture and altitudinal dependence, I believe that setting up the subject more clearly would assist with the delivery of the major findings. That is, I would suggest text along the lines of: "In this study, I investigate the various altitudinal effects (i.e., thermal cycling, snow cover, ice segregation) on rock fracture and place these in the context of climate change." On this last notion, climate change is discussed in the manuscript, but really only casually at the end and I feel that to tackle this subject, the Discussion should include a more in depth overview of what others have found on this subject. Referring back to the Abstract, I noted that the Conclusions section is almost exactly the same as the Abstract. Please note that the Abstract should provide an overview for readers who have not yet read the paper. The Conclusion summarizes the work for those readers who have finished reading the paper. They should therefore not contain the same identical content. Finally, regarding the overall structure of the manuscript, I found the Results and parts of the Discussion section quite tedious within the overall presentation. Whole sections of the text could be summarized in a table or chart, and it is not necessary to highlight the results of every fracture measurement or temperature reading. I therefore recommend a rewrite of large sections of the text (including the Abstract, Results, Discussion, and Conclusion) so that the results and main findings of the research are more clearly represented. Overall, I found the manuscript did not clearly deliver the apparent intended results of the study.

I like to thank the reviewer for his/her valuable comments. I can understand that the structure and the detailed writing overshadow the main messages of the manuscript. To clarify my intended results, I followed the recommendations of the reviewer and revised the manuscript significantly.

The reviewer criticized the abstract and recommended a revision and a clear setting up of the objectives in the abstract. I completely rewrote the abstract and shortly introduced the geomorphic context: "In alpine environments, tectonic processes, past glaciation and weathering processes fractured rock and prepare or trigger rockfalls, which are important processes of rock slope evolution

and natural hazards." This sentence followed a text that introduce the objectives: "In this study, I quantify thermal- and ice-induced rock and fracture kinematics and place these in the context of their role in producing rockfall and climate change." Then, I shortly introduced the applied techniques and research set up: "I conducted laboratory measurements on intact rock samples, and installed temperature loggers and crackmeters at four rockwalls reaching from 2585 to 2935 m in elevation in the Hungerli Valley, Swiss Alps." and summarized the main findings: "My laboratory data shows that thermal expansion followed three phases of rock kinematics, which resulted in a hysteresis effect. In the field, control crackmeters on intact rock reflected these temperature phases and based on thermal expansion coefficients of these observed phases, I modelled thermal stress. Model results show that thermal stress magnitudes were predominantly below rock strengths. Crackmeters across fractures revealed fracture opening during cooling and reverse closing behaviour during warming on daily scale. Elevation-dependent snow cover controlled the number of daily temperature changes and thermal stresses affecting both intact and fractured rock, while the magnitude is controlled by topographic factors influencing insolation. On seasonal scale, slow ice segregation induced fracture opening can occur within lithology-dependent temperature regimes called frost cracking windows. Shear plane dipping controlled if fractures opened or closed irreversible with time due to thermal-induced block crawling on annual scale." before setting my findings in the larger context of rockfall and climate change: "Climate change will shorten snow duration and increase temperature extremes, therefore, will affect the number and the magnitude of thermal changes and associated stresses. Earlier snowmelt in combination with temperature increase will shift the ice-induced kinematic processes to higher altitudes. In conclusion, climate change will affect and change rock and fracture kinematics and, therefore, change rockfall patterns in Alpine environments." and providing a direction for future work: "Future work should quantify rockfall patterns and link these patterns to climatic drivers. "

To improve the structure and overall tedious representation, I rewrote the result and discussion section. I added a thermal stress model to increase the attention of a wider readership as demanded by Reviewer 2. I changed my style of writing, focused on my key findings, and omitted details that are not necessary to understand the main messages of my manuscript. The aim of my laboratory test was to identify trajectories of thermal-induced rock deformation. The control crackmeters were used to validate these trajectories in the field. I used the thermal expansion coefficients of the laboratory measurements in combination with added rock temperature loggers to drive a thermal stress model. I validate the model results using Schmidt hammer measurements. I added the required information on the research set up in the method section:

"To monitor rock surface temperature (RST), I installed four Maxim iButton DS1922 L temperature loggers with a nominal accuracy of ±0.5 °C in 10 cm deep boreholes following the measurement method by previous studies (e.g. Draebing et al., 2017a; Haberkorn et al., 2015). The loggers recorded RST in 3h intervals between 1 September 2016 and 31 August 2019 (RW1-3) or between 1 September 2017 and 31 August 2019 (RWS), respectively. Due to the logger location in 10 cm depth, I determined snow cover duration using the uniform standard deviation threshold of <0.5 K for positive and negative RST in accordance to Haberkorn et al. (2015). I calculated daily rock temperature warming and cooling cycles ΔRT and applied the equation from Anderson and Anderson (2012) to model thermal stress σ_{th}:

$\sigma_{th} = \frac{\alpha\, E\, \Delta RT}{(1-\upsilon)}$."

In addition to the more general comments on the result section, the reviewer stated some specific comments:

Results. Many pages of the results are tedious to read and are presented as detailed descriptions of the exact deformation and temperature changes that the laboratory and field rocks went through. For example, most of Section 4.1 and nearly all of Sections 4.2.3 and 4.2.4 (which encompasses _ 2 pages of text) could be summarized in a few generalized sentences that describe the results in a chart form. The idea here is to ensure that the reader is guided through the results and their meaning instead of needing to interpret them on their own. As presented, it is not clear what the meaning is of the numerical values presented, other than a description of some parts of the figures.

and

Figures. Whereas this study is clearly complex with bringing together observations from both a laboratory setting and several field sites, I am not sure that there is a need to present all the data for all of the sites in all of the figures. For example, Fig. 4 presents what appears to be similar data for both cracks at RW-1. If this is the case, only one plot could be presented and the other could be moved to the supplementary information. The idea is that if the data does not add to the story, than it does not necessarily need to be presented in the main text. For those scientists interested in using the data, the supplementary information could be consulted. This could also apply to Figs. 6, 7, 8, and 10. As currently presented, the take-home message of the presented results is not clear. On this note, I believe that more detailed captions could assist with describing the salient aspects and findings of the study.

I restructured the result section into three parts, shortened the result section significantly, merged figures and added more information in the caption to describe the figures. The first part presents the "Meteorological conditions and rock surface temperatures". The section on the rock surface temperatures are new:

"Rock surface temperatures (RST) followed the annual and daily oscillation of air temperatures. At annual scale, RST of north-exposed rockwalls ranged from -12.9 °C up to 13.4 °C for RW1, -5.6 °C up to 17.6 °C for RW2 and -7.0 °C up to 13.9 °C for RW3 (Fig. 4b-d). In contrast, the south-exposed logger at RWS recorded higher RST variations between -12 °C and 32 °C (Fig. 4e). At daily scale, the north-facing loggers measured small daily temperature variations up to 4 °C, whereas the south-exposed logger recorded variations up to 16.5 °C. Snow cover attenuated daily temperature oscillations with expected high deviation between north- and south-exposed rockwalls. At north-facing rockwalls, snow cover onset was between October and November and lasted between 220 days and 251 days per year with only minor differences between RW1 to RW3 and individual years (Fig. 4b-d, Table 3). In contrast, snow onset was delayed to mid- February 2018 or snow cover was only sporadic in 2019, therefore, snow cover duration was reduced to 5to 80 days (Fig. 4e)." I also added a new figure presenting the results:

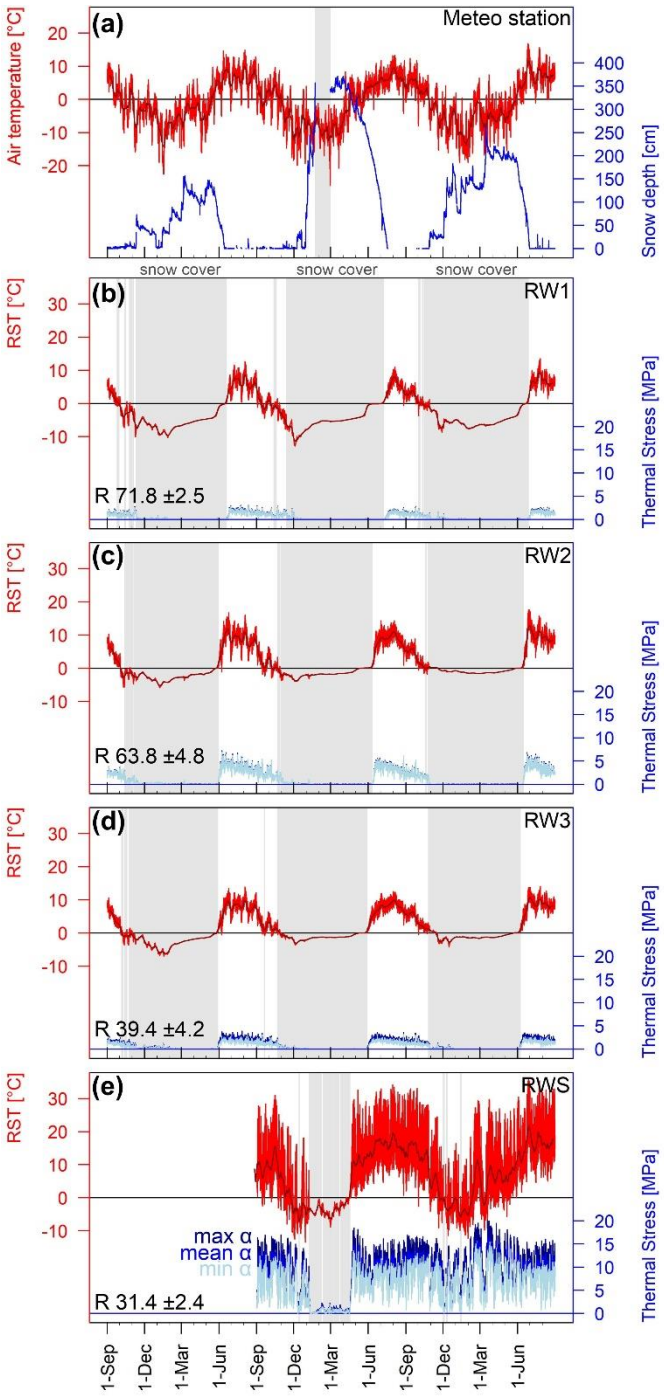

Figure 4: (a) Air temperature and snow depth from meteo station Oberer Stelligletscher plotted for the period from September 2016 to August 2019. Rock surface temperatures (red lines) and mean 10-day RST (dark red line) recorded by iButtons installed at (b) RW1, (c) RW2, (d) RW3 and (e) RWS. Thermal stress was modelled using minimum α (light blue lines), mean α (blue lines) and maximum α (dark blue lines) Grey rectangles highlight the data gap filled with modelled air temperatures in (a) and snow cover (b-e). Numbers represent measured Schmidt hammer rebound values R.

The second section “Laboratory and field rock deformation and resulting stresses” focusses on the results of the laboratory tests, the control crackmeters and the thermal stress model. Following the reviewer comments, I merged Fig. 4 and 5 to one new Figure 5 representing the major findings of laboratory tests and control crackmeter:

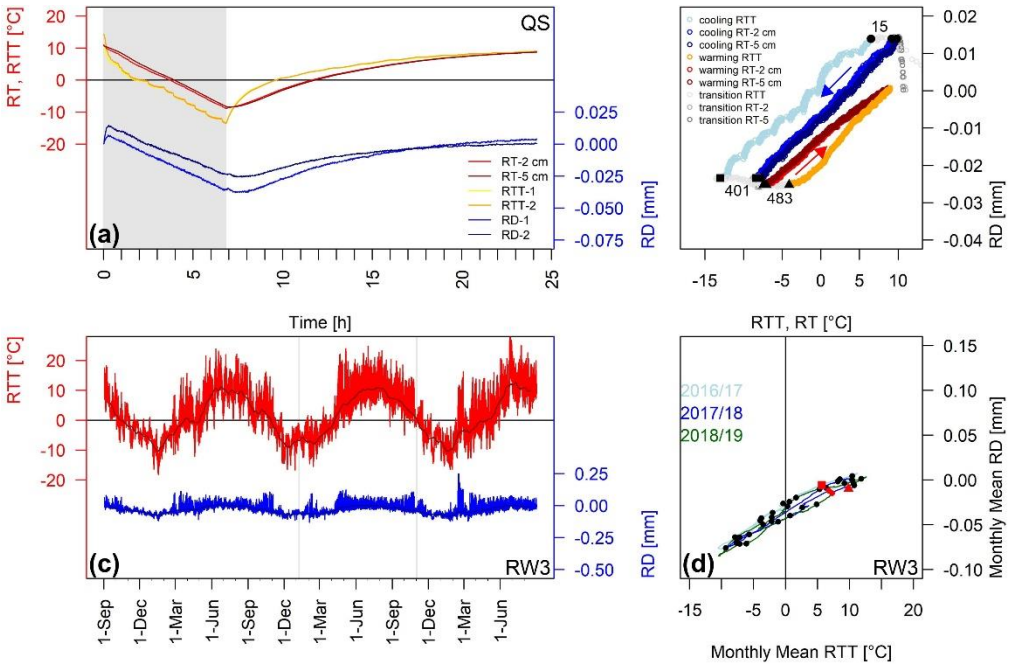

Figure 5: Laboratory crackmeter measurements of rock samples. (a) Rock-top temperature (RTT), rock temperature (RT) and rock deformation (RD) of crackmeter 1 and 2 plotted versus time for the schistose quartz slate sample (QS). (b) Rock deformation plotted versus rock-top temperature or rock temperature for crackmeter 2 of QS. Numbers indicate the timing of the beginning of the cooling period (black dot), end of the cooling period (black rectangle) and beginning of the warming period (black triangle). Arrows highlight the temporal trajectory of cooling (blue) and warming (red). Results of all laboratory measurements are shown in Fig. S1 and S2 in the supplementary information. Field measurements of the control crackmeter at RW3. (c) RTT (red line) and monthly mean RTT (dark red line), RD (blue line) and monthly mean RD (dark blue line) plotted versus time for the period from 1 September 2016 to 31 August 2019. Grey rectangles highlight the occurrence of snow cover. (d) Monthly mean rock deformation plotted versus monthly mean RTT. Red rectangles indicate start, black dots first day of a month, red dots the beginning of new measurement period and red triangles the end of measurements. Colour of graphs indicate data from 2016/17 (light blue), from 2017/18 (blue) and 2018/19 (green). For results of RW1 and RWS, see Fig. S3 in the supplementary information.

I rewrote the text to highlight the main findings:

"Directly after the start of cooling, several crackmeters revealed a rock expansion, which lasted for a few minutes (initial transition phase; Fig. 5a and Fig. S1c, e-f). Rock samples were cooled down to a RTT between -13.2 °C and -18.4 °C and all crackmeters experienced a negative RD (Fig. 5a-b, Fig. S1-2). Rock temperature in 2 to 5 cm depth was up to 5 to 7 °C higher than RTT during the cooling phase (Fig. 5 and S1-2). Based on $RT_{5\,cm}$ measurements using Eq. (1), thermal coefficient ranged from 5.8 ±0.0 10^{-6} $°C^{-1}$ for AM (r^2=1) to 7.3 ±0.2 10^{-6} $°C^{-1}$ (r^2=0.99) for AP and 7.3 ±0.5 10^{-6} $°C^{-1}$ (r^2=1) for QS during cooling. Nine to 23 min after stopping cooling, several crackmeters at all rock samples (AP RD_2, AM RD_2, QS RD_1 and RD_2) experienced a sudden rock deformation ranging from +0.004 mm to +0.0135 mm (transition phase; Fig. 4b, Fig, S2). Despite an increase of RTT from -7.3 to -5 °C, the QS sample and AP RD_1 and AM RD_1 showed a further rock contraction between -0.0016 mm and -0.0032 mm. The closing behaviour corresponded to the decrease of $RT_{5\,cm}$ from -8.2 °C to -9.3 (Fig. 4b). Subsequent warming up to 7.7 or 8 °C RTT resulted in rock expansion (warming phase, Fig. 5a-b and S1-2). This warming phase induced a thermal expansion that corresponds to a thermal expansion coefficient of 7.5 ±0.4 10^{-6} $°C^{-1}$ (r^2=1) for AP, 7.0 ±0.2 10^{-6} $°C^{-1}$ (r^2=1) for AM and 7.1 ±1.7 10^{-6} $°C^{-1}$ (r^2=0.99) for QS. All samples showed a hysteresis effect during warming and cooling cycles (Fig. 4b, Fig. S2), which was amplified using RTT and decreased with further rock temperature depth from $RT_{2\,cm}$ to $RT_{5\,cm}$.

Control crackmeters were installed in the field to validate laboratory-observed rock deformation. RTT fluctuated between -15 °C and 10 °C at RW1 in 2017/18, between -20 °C and 25 °C at RW3 from 2016 to 2019 and from -15 °C to 25 °C at RWS from 2017 to 2019 (Fig. 5c, Fig. S3). All control crackmeters showed small daily fluctuations of rock deformation that were even reduced when snow cover

occurred. Similar to laboratory experiments, control crackmeters recorded cyclic rock expansion during warming and contrary rock contraction during cooling periods (Fig. 5 d, Fig. S3). The thermal expansion coefficients for cooling and warming based on monthly mean RD and RTT was 6.5 10^{-6} $°C^{-1}$ for RW1 (r^2 = 0.43), 9.4 10^{-6} $°C^{-1}$ for RW3 (r^2 = 0.94) and 9.0 10^{-6} $°C^{-1}$ for RWS (r^2 = 0.9). All control crackmeters showed a hysteresis effect, which was amplified at RW1.

Applying laboratory derived thermal expansion coefficients (Table 1) for warming and cooling to Eq. (2) provides the daily thermal stresses within a rockwall. Daily thermal stresses reflected RST and were increased during snow-free periods in summer and decreased or absent during snow cover periods. Maximum stresses reached up to 2.9-3.0 MPa at RW1, 6.8-7.2 MPa at RW2, 3.1-3.9 MPA at RW3 and 15.4-20.1 MPa at RWS (Fig. 4b-e).“

The third part of the result section “Rockwall fracture kinematics” presents the main results of the crackmeters spanning fractures. I significantly shortened the text from two to less than one page. I identified four phases, highlighted these phases in Figure 6 and used these phase to structure the result section:

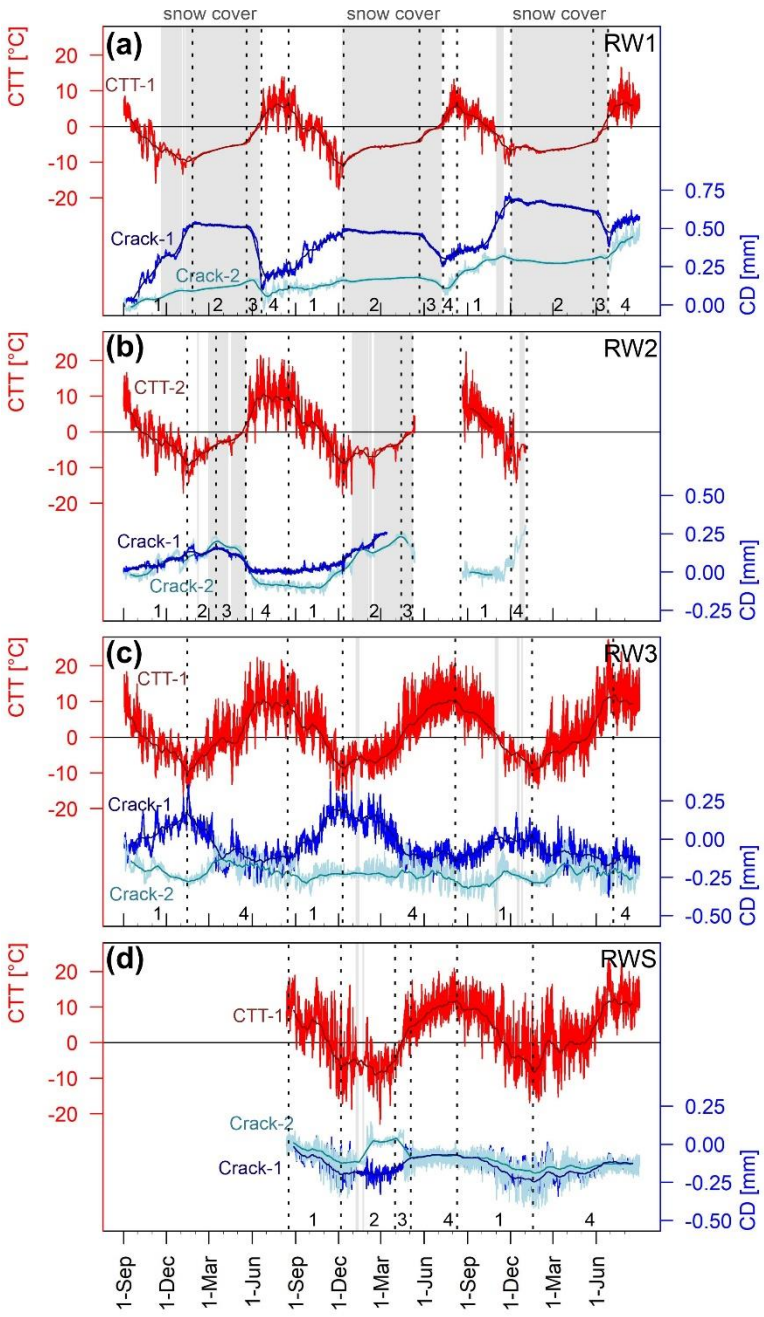

Figure 6: Crack-top temperature, monthly mean crack-top temperature, crack deformation and monthly mean crack deformation for the crackmeters at (a) RW1, (b) RW2, (c) RW3 and (d) RWS for the period 1 September 2016 to 31 August 2019. Grey rectangles highlight the snow cover period, while numbers indicate the interpreted phases (see Table 4).

I omitted the details of fracture movement from the text and present these details now as a new table structured following the four identified phases:

Table 4: Quantified rock fracture kinematic phases, annual and overall crack deformation in mm. Crack deformation (CD) is differentiated in crack closing (-), crack opening (+) and no CD (±).

Phases/	RW1		RW2		RW3		RWS	
Cumulative crack deformation	Crack-1	Crack-2	Crack-1	Crack-2	Crack-1	Crack-2	Crack-1	Crack-2
Phase 1: cooling period								
2016-17	+0.53	+0.09	+0.13	+0.09	+0.17	-0.28		
2017-18	+0.22	+0.04			+0.33	+0.01	-0.20	-0.12
2018-19	+0.32	+0.08			+0.15	±0.00	-0.18	-0.10
Phase 2								
2017	-0.05	+0.07	+0.02	+0.11				
2018	+0.02	+0.03						+0.16
2019	-0.08	-0.01						
Phase 3								
2017	-0.31	-0.10	-0.15	-0.29				
2018	-0.18	-0.07						-0.13
2019	-0.12	+0.03						
Phase 4: warming period								
2017	+0.07	+0.05			-0.31	+0.04		
2018	+0.06	+0.12			-0.33	-0.05	+0.14	±0.00
2019	+0.06	+0.11			-0.13	-0.04	+0.13	+0.08
cumulative annual CD								
2016/17	+0.24	+0.11	±0.00	-0.10	-0.09	-0.24		
2017/18	+0.12	+0.12			-0.02	-0.08	-0.06	-0.09
2018/19	+0.20	+0.22			-0.13	+0.07	-0.03	-0.04
overall CD	***+0.56***	***+0.45***			***-0.24***	***-0.25***	***-0.09***	***-0.13***

In my result section, I now focus on the main findings:

"Crackmeters showed a decrease of snow duration with decreasing elevation. Crackmeters at RW1 located at 2935 m experienced 192 to 223 days of snow cover per year (Fig. 6). The number of snow-covered days was reduced to 69 and 73 days in 2016/17 at RW2 at 2672 m. Snow load damaged the equipment in the following years, which resulted in a data gap and incomplete measurement of snow cover duration. RW-3 at 2585 m showed between zero and nine days of snow cover and snow cover was limited to two days at Crack-2 in 2017/18 at the south-facing rockwall RWS.

All crackmeters experienced a cooling period (Phase 1 in Fig. 6) that ranged from September until mid-December to Mid-February. At RW1, the onset of snow cover controlled the end of the cooling period, only in 2016/17 cooling continued under snow cover. The cooling period was characterized by a crack opening (Table 4), which was between 0.22 and 0.53 mm at Crack-1 and between 0.04 and 0.09 mm at Crack-2 at RW1. At RW2, cracks opened between 0.09 mm at Crack-2 and 0.13 mm at Crack-1, while Crack-1 at RW3 revealed a crack opening between 0.15 and 0.33 mm. In contrast, Crack-2 at RW3 experienced a diverse crack deformation ranging from crack closing between 0.28 mm to 0.01 mm crack opening. At RWS, the cooling period was characterized by crack closing between 0.18 and 0.20 mm at Crack-1 and between 0.1 and 0.12 mm at Crack-2.

At RW1 and RW2, crackmeters experienced a slow warming below snow cover (Phase 2 in Fig. 6), which resulted in either crack opening or crack closing (Table 4). Crackmeters at RW1 experienced a crack deformation ranging from closing of 0.08 mm to crack opening of 0.07 mm. At RW2, cracks experienced

a crack opening between 0.02 and 0.11 mm. At RWS, snow cover was absent during warming, however, Crack-2 experienced an opening of 0.16 mm, which was reversed by 0.13 mm during enhanced warming in 2017. RW1 and RW2 showed a period of predominantly crack closing during enhanced warming until snow cover completely melted (Phase 3 in Fig. 6). Crack-1 at RW1 experienced between 0.12 to 0.31 mm crack closing, while Crack-2 showed a diverse crack deformation ranging between 0.03 mm opening and 0.10 mm closing. At RW2, the crackmeters revealed crack closing between 0.15 and 0.29 mm.

All crackmeters experienced a warming period (Phase 4 in Fig. 6), which is characterized by both crack closing and crack opening (Table 4). At RW1, crackmeters revealed a crack opening between 0.05 and 0.12 mm. In contrast, RW3 showed a crack closing between 0.13 and 0.33 mm at Crack-1 and a crack deformation behaviour ranging from 0.07 crack opening to 0.24 mm crack closing at Crack-2. At RWS, the warming period is associated with crack opening between 0.00 and 0.14 mm. In the 3-year period, RW1 experienced a crack opening between 0.45 and 0.51 mm. In contrast, RW3 showed an overall crack closing between 0.24 and 0.25 mm. Data at RW2 was limited to 2016/17 and cracks experienced no change or 0.1 mm closing. RWS was characterized by crack closing in each year with a cumulative closing between 0.03 and 0.09 mm.

On a daily scale, cooling resulted in crack opening due to contraction of two rock blocks and warming in crack closing due to expansion of two rocks (Fig. 8). The peak of opening and closing between individual crackmeters can be different. Crackmeters at RW1 experienced daily CTT fluctuations in the range below 10°C and daily CD below 0.1 mm (Fig. 9) during snow-free periods. The fluctuations were increased up to 16°C and 0.11 mm at RW2, 23 °C and 0.26 mm at RW3 as well as 21°C and 0.32 mm at RW-S."

The reviewer suggested that subfigures from Figures 7 and 8 can be potentially moved to the supplementary information. Here, I disagree. The differences between the crackmeter kinematics result from different insolation that alters rock temperatures and different insulation from snow cover. These effects become visible when all crackmeters from different altitudes and different aspects are displayed.

I understand that the major pattern of daily temperature magnitudes are visible in one year and I reduced the number of subfigures in former Fig. 10 and moved the former figure to the supplementary information:

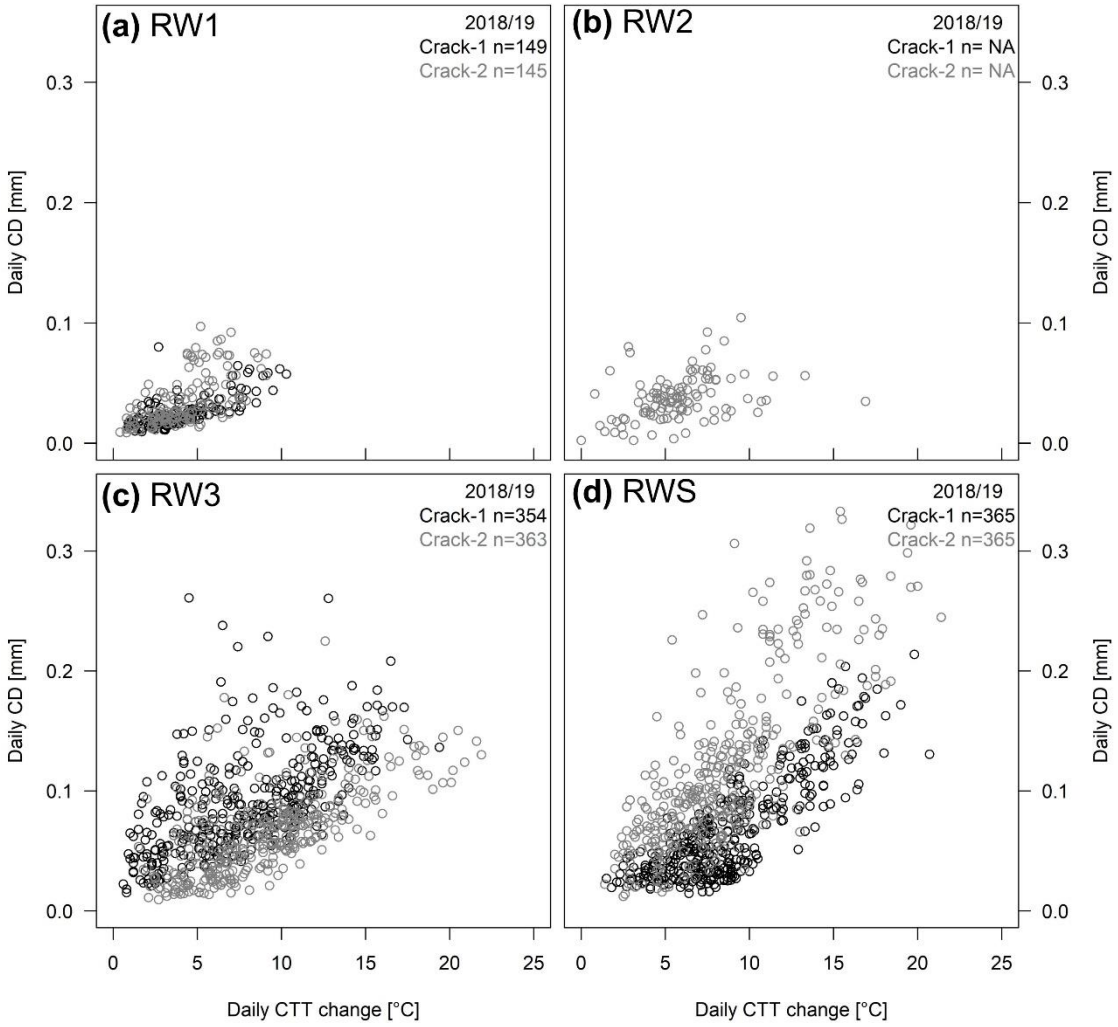

Figure 9: Daily crack deformation plotted versus daily crack-top temperature for (a) RW1, (b) RW2, (c) RW3 and (d) RWS in 2018/19. Numbers n indicate the number of daily cycles, NA highlights incomplete measurements during the period due to instrument failure. For results of all periods, see Fig. S5 in the supplementary information.

According to the reviewer: "the Discussion should include a more in depth overview of what others have found on this subject". Furthermore the reviewers suggests a revision: " On a final note, I found Fig. 11 quite interesting and would recommend that this figure be used to structure the large part of the Discussion section."

The reviewer's specific comment include:

"Discussion. I found the Discussion section lacking in overall applicability to the geomorphological community at large. Typically, discussion sections try to place the context of the study in relationship to existing work. The author does that to some degree, but mostly only to their own previous publications. I would have liked to see the results compared to those from other researchers working in this field and also to what they think is the likelihood that these results apply to other mountainous settings. In addition, placing the climate change interpretations in the context of others working on similar research in mountainous settings (e.g., Ravenel, Gruber, and others) would also provide the broader applicability that could make this research more impactful. Finally, much of the Discussion (large parts of Sections 5.1 and 5.2, which again span several pages) appear to be a continuation of the intricately detailed results. The Discussion is the section that allow the results to be placed into context, but I did not find this to be the case."

I can understand the comments and restructured the discussion following the reviewer's recommendation using former Fig. 11 (Fig. 10 in the revised version). I shortened the discussion of the laboratory tests and control crackmeters from two to one pages and omitted the repetitive presentation of the results. In contrast, I focussed more on my main findings, the existence if the three phases: warming, transition and cooling phase:

„5.1 Cyclic thermal rock deformation

Cyclic thermal stresses can result in thermal fatigue that breakdown rock and is an important component of mechanical weathering. In my laboratory tests, I can differentiate thermal cycles into three phases: (1) cooling phase, (2) transition phase, (3) warming phase. The (1) cooling phase was characterized by rock contraction with thermal coefficients α (Table 1), which are in the order of previous thermal expansion coefficients for quartz minerals (Siegesmund et al., 2008) or rock samples (Ruedrich et al., 2011; Skinner, 1966). After stopping cooling and enhancing a natural warming of the rock samples, the (2) transition phase started (Fig. 5a-b). Some crackmeters experienced a sudden rock deformation due to rapid rock response to warming, while other crackmeters even on the same rock sample showed further rock contraction (Fig. S1-2). The contraction behaviour corresponded to decreasing $RT_{5\ cm}$, while RTT was already increasing as a response to warmer air temperature. Therefore, the transition phase is characterized by a temperature difference between rock surface (RTT) and rock depth (RT_{5cm}), which is a result of the slow speed of heat conduction. While the rock surface (RTT) was warming and rock was expanding, the overall rock kinematics was still controlled by cooling of the rock interior and associated contraction. The (3) warming phase was characterized by rock expansion (Fig. 4 and 5) with thermal expansion coefficients that are slightly different from the cooling (Table 1). Therefore, thermal cycles showed a hysteresis effect, which was previously observed on other lithologies (Ruedrich et al., 2011).
The control crackmeters demonstrated that snow cover controls the occurrence of daily temperature cycles, and associated rock expansion during warming and contrary rock contraction during cooling. Daily temperature changes affected the upper 0.21 to 0.42 m assuming a 12 h temperature cycle and a thermal diffusivity between 1 and 2 mm s^{-2} typical for metamorphic rocks (Vosteen and Schellschmidt, 2003; Cermák and Rybach, 1982). These rock depths correspond to daily temperature cycles in rockwalls observed in previous studies (Gunzburger and Merrien-Soukatchoff, 2011; Anderson, 1998). On annual scale, thermal changes affected 4 to 8 m and, therefore, the entire instrumented rock blocks assuming a half-year cycle and thermal diffusivities typical for metamorphic rocks. Rock temperature boreholes in the Alps suggest heat propagation to similar depths (Phillips et al., 2016a; PERMOS, 2019). Control crackmeters revealed identical phases of thermal-induced rock deformation as laboratory measurements including hysteresis effects. The hysteresis effect was amplified at RW-1, where rock blocks are between 2 and 4 times larger than rock blocks at the other rockwalls (Fig. 3). A larger rock block size results in a longer heat transfer by conduction and increases the transition phase, therefore, I interpret the increase of the hysteresis effect as a result from block size and an effect of scale. The observed differential thermal expansion in combination with different response during transition phase results in mechanical stresses able to breakdown rock that will be discussed in Chapter 5.3."

In section 2 of the discussion section, I focus on the fracture kinematics and put my results in the context of previous studies. I also shortened this section by 50%. Most studies focused on sheeting joints where progressive rock movement can trigger rockfall in terms of toppling or wedge failures. However, not all moving blocks are located in steep or overhanging rockwalls but these blocks can progressively move by identical processes as demonstrated by my data and the thermal- and ice-induced movement can also result in rockfall.

"In overhanging steep rock cliffs, thermal stresses can propagate fractures and trigger rockfall (Collins and Stock, 2016; Stock et al., 2012). Exfoliation joints warm differentially (Guerin et al., 2019) and thermal bowing results in fracture propagation parallel to the rockwall (Collins and Stock, 2016). In fractured rock, daily and annual thermal cycles result in rock contraction with fracture widening during cooling and rock expansion during warming with fracture closing (Fig. 11b; Cooper and Simmons, 1977; Draebing et al., 2017b). My data showed that crack opening and closing occurred on a daily scale (Fig. 8). The magnitude of this crack deformation depends on the magnitude of temperature change and was increased at RWS and RW3, which experienced much higher daily temperature changes (Fig. 9). The data demonstrated that the number of daily temperature changes per year (Fig. 9 and Fig. S5) is controlled by the duration of snow cover. Snow cover insulates the ground (Zhang, 2005) and decreases daily thermal changes (Fig. 10; Luetschg and Haeberli, 2005; Draebing et al., 2017b), therefore, rockwalls at lower elevations (e.g. RW3) or south-exposed rockwalls (e.g. RWS) experienced a shorter snow cover duration (Table 2) and a higher frequency of thermal cycles than higher-elevated rockwalls with longer snow cover (e.g. RW2-3).

On seasonal scale, several crackmeters experienced a slow crack opening during negative CTT that suggest the influence of ice (Fig. 11c). Matsuoka (2001, 2008) observed rapid crack opening during freeze-thaw cycles in spring or autumn that suggest volumetric expansion as the trigger of crack opening. In contrast, I observed a slow crack opening lasting between 1.5 to 2 months at RW2 in 2017 (Fig. 6b and Fig. 7c-d), 3 to 3.5 months at Crack-2 at RWS in 2018 (Fig. 6d and Fig. 7h), and 5 to 5.5 months at Crack-2 at RW1 in 2017 and 2019 (Fig. 6a and Fig. 7b). The opening occurred in a CTT range between -5 to -3.3°C at RW2, between -8 and -3.6°C at RWS and -9 to -1°C at RW1. These temperature ranges are within the frost cracking window from -8 to -3 °C suggested by Anderson (1998) or in the range of laboratory observed frost cracking windows of aplite, amphibolite and schist quartz slate (Draebing and Krautblatter, 2019). The temporal trajectories of the affected cracks showed that crack opening occurred during warming within the negative temperature range (Fig. 7b-d. h), therefore, a purely thermal response of the rock would result in rock expansion and crack closing. In addition, a transition phase as observed in the laboratory or at control crackmeters can be excluded, thus, the transition phase is associated with temperature changes from warming to cooling or reverse, which were absent during these crack opening phases. Therefore, I interpret the observed crack opening as a result of ice segregation and subsequent closing because of ice relaxation. Cracks can infill with ice by refreezing of meltwater, ice infill growth slowly with time by cryosuction (Weber et al., 2018; Draebing et al., 2017b) and build up ice pressure and stresses in a subcritical range (Draebing and Krautblatter, 2019), which induce slow fracture opening (Draebing and Krautblatter, 2019; Draebing et al., 2017b).

On annual scale, thermal-induced crack opening and closing can be reinforced by cryogenic processes (Hasler et al., 2012), can propagate fractures (Ishikawa et al., 2004) and can result in irreversible rock movement (Weber et al., 2017). Previous studies focussed on toppling rock blocks (Ishikawa et al., 2004) or provided no information on the failure type (Hasler et al., 2012; Weber et al., 2017). Due to the tectonic setting, the observed blocks are located on a shear plane dipping out of the slope (RW1-2, Fig.3 a) or dipping into the slope (RW3, RWS; Fig. 3b-d). Gunzburger et al. (2005) observed daily non-permanent block movement and suggested that thermal changes can induce rock creep along shear planes. On non-buttressed blocks located on shear planes dipping out of the slope (RW1), crackmeters recorded annual and overall crack opening indicating that the lower located block in Figure 3 a is creeping slope downwards with an annual rate of 0.11 to 0.24 mm a^{-1} (Table 4). The majority of the creeping occurred during the cooling phase (Phase 1 in Fig. 6a), which was characterized by 0.22 to 0.53 mm opening of Crack-1 at RW1. This opening was slightly reversed at Crack-1 and extended at Crack-2 by ice segregation during phase 2. In Phase 3, the closing pattern reversed most of the previous crack opening. The warming phase 4 induced a crack opening, which is contrary to expected crack

closing. Bakun-Mazor et al. (2020) identified thermally-induced wedging as a cause of crack opening during warming. The rock contracts during cooling and a wedge within the fracture sinks into the cooling-induced gap and causes a crack opening during warming induced thermal expansion. A wedge was not visible at Crack-1 and the annual opening exceed the crack opening during the warming phase 4. Therefore, I interpret the crack opening as irreversible thermal-induced block movement.

In contrast to RW1, all other block are located on shear planes dipping into the rockwall or buttressed by other blocks (Fig. 3b-d). The cooling phase resulted in crack opening at RW2 and Crack-1 at RW3 and the opening was reversed during the warming phase 4 resulting in an irreversible annual (RW2-3) and overall closing (RW3). Crack closing at Crack-2 at RW3 and RWS occurred during the cooling period and was not completely reversed during the warming period resulting in an annual and overall crack closing (Table 4). In summary, thermal induced crack deformation caused an irreversible block movement along the shear plane into the rockwall (Fig. 11e)."

Furthermore, I placed my results on climate change into a context presented by previous studies. I modelled thermal stresses and link my model results and daily fracture kinematics with previous studies focusing on mechanics and climate change:

"Thermal changes are an important climatic factor inducing stresses responsible for mechanical weathering (Eppes and Keanini, 2017). Thermal stresses cause subcritical cracking (Eppes et al., 2016) and propagate fractures (Eppes et al., 2010; Eppes and Keanini, 2017). In alpine rockwalls, thermal changes result in deformation of rocks (Guerin et al., 2020; Collins and Stock, 2016) and induced stresses can decrease the strength of stability-relevant rock bridges (Guerin et al., 2019) and can trigger rockfall (Stock et al., 2012; Collins and Stock, 2016). Applying the observed thermal coefficients and recorded RST in 10 cm depth to the thermal stress model by Anderson and Anderson (2012) demonstrated that thermal stresses occurred during snow-free periods and during periods of thin snow cover before snow achieved sufficient height to insulate the rock surface (Phillips, 2000; Luetschg and Haeberli, 2005). Modelled thermal stresses represent maximum values, thus, the equation (2) assumes isotropic material and an equal volumetric expansion in every direction. Occurring rock types possess cracks and schist planes, which results in anisotropy ranging between 0.05 for amphibolite, 0.06 for aplite and 0.55 for schistose quartz slate (Draebing and Krautblatter, 2019). Therefore, modelled stresses for schistose quartz slate are potentially overestimated. Stresses will concentrate at crack tips and widen cracks (Eppes and Keanini, 2017), however, stress calculation requires knowledge on crack geometry which is not available. The applied model provides a quantitative measure of stress levels and demonstrates that stresses occurring at RW1-3 are below tensile strengths and compressive strengths of in-situ rock (Table 1). Thermal stresses are not exceeding rock strength and are subcritical in sensu Eppes and Keanini (2017), however, the cyclicity of thermal stresses progressively weakens rock (Eppes et al., 2016). Schmidt hammer values showed high values between 63 ±4.8 and 71.8 ±2.5 for RW1-2, which consist of high-strength aplite and amphibolite (Table 1), therefore, these values suggest minor weathering near the surface. In contrast, rockwalls with schistose quartz slate revealed lower rebound values with RWS had lower (31.4 ±2.4) values than RW3 (39.4 ±4.2). This could be a result of higher modelled thermal stresses at RWS compared to RW3 (Fig. 4). However, thermal processes are not acting isolated and other weathering processes including mechanical, chemical and biological weathering can be responsible for the observed decrease in rock strength (Viles, 2013b; Eppes and Keanini, 2017). As soon cracks are existent, daily thermal changes induce fracture kinematics that can widen cracks (Fig. 10b). My data demonstrated that snow cover controls the number of daily crack deformation (Fig. 8 and Fig. S5). According to Bender et al. (2020), the changes of snow duration is elevation dependent and locations in Valais above to 2500 m will experience a shortening of the snow season of approximately 10 % by 2035, 17 % by 2060 and 25 % by 2085. Temperature extremes and variability (Schär et al., 2004; Gobiet et al., 2014) will increase in the future.

Therefore, the number and the magnitude of thermal stresses will increase in the future, which could be amplified if climate becomes wetter (Eppes et al., 2020). Consequently, thermal stresses will play a more important role in preparing and triggering rockfall in the future."

Then I focus on cryogenic fracture displacement and put my results into the context of the frost cracking window and potential altitudinal shifts of this window due to climate change:

"Cryogenic processes can cause fracture movement (Draebing et al., 2017b) and produces subcritical stresses that are below tensile strengths of rocks (Draebing and Krautblatter, 2019). These stresses occur in a wide temperature range between -15 and -1°C according to field measurements (Girard et al., 2013; Amitrano et al., 2012), numerical models (Walder and Hallet, 1985) and laboratory tests (Draebing and Krautblatter, 2019). My data showed the occurrence of cryogenic induced opening and closing at several crackmeters (Fig. 7b-d, 7h). The slow opening in combination with the temperature regime suggests that ice segregation is the driving process behind the observed crack opening. This opening can progressively weaken rockwall strength and potentially triggers rock slope failure as observed at Piz Kesch in winter 2014 (Phillips et al., 2016b). The length of the temperature window enabling ice segregation increases with altitude but is modulated by insulating snow cover. Climate change will shorten the snow duration by an earlier meltout date (Bender et al., 2020) and increase air and ground temperatures (Bender et al., 2020; Gobiet et al., 2014), therefore, the time period of temperature windows enabling ice segregation will decrease. This will affect especially rockwalls located at lower elevations, therefore, cryogenic processes and triggered rockfall will be shifted to higher elevations. At higher-elevations, the climate-changed induced changes of the temperature regime will also affect permafrost rockwalls, decrease rockwall stability (Draebing et al., 2014; Krautblatter et al., 2013) and increase rockfall activity due to increased thawing (Ravanel et al., 2010; Ravanel and Deline, 2010) amplified by temperature extremes (Gruber et al., 2004b; Ravanel et al., 2017)."

Finally, I focus on observed rock creeping, which is controlled by geology and put my results into a wider context of rock slope movement or deep-seated gravitational slope deformations:

"Plastic deformation of fractures contributes to the preparation of rockfalls (Gunzburger et al., 2005). Previous studies demonstrated that thermal-induced crack deformation causes irreversible displacement of rock blocks (Weber et al., 2017; Hasler et al., 2012). Gunzburger et al. (2005) and do Amaral Vargas et al. (2013) suggested that thermal changes can cause rock creep along shear planes. My data demonstrates that rock blocks creep with a direction depending on shear plane dipping. Dipping out of the rockwall results in creeping that increases fracture opening (RW1, Fig. 10d) and can trigger rockslide processes. In contrast, dipping into the rockwall causes fracture closing (RW3, RWS; Fig. 10e). My observed blocks will not be released as rockfall, however, the observed mechanism can trigger a wedge failure in more steeper and overhanging rockwalls that are more susceptible to rockfall (Matasci et al., 2017). Several studies indicated that thermal-induced stresses can affect rock slopes up to 100 m depth (Gischig et al., 2011b) and affect deep-seated gravitational slope deformations (Gischig et al., 2011a; Rouyet et al., 2017; Watson et al., 2004). Therefore, thermal changes can decrease rock slope stability with time (preparatory factor) and potentially cause landsliding (triggering factor)."

The reviewer commended that: "Conclusions section is almost exactly the same as the Abstract. Please note that the Abstract should provide an overview for readers who have not yet read the paper. The Conclusion summarizes the work for those readers who have finished reading the paper. They should therefore not contain the same identical content."

I rewrote the conclusion section and omitted all sentences on the set up and methods that the reader already knows and focused on the main findings:

"Thermal-induced rock deformation can cause fracture movement and thermal stresses able to breakdown rock. Cyclic thermal rock deformation follows a cooling and warming phase with different thermal expansion coefficients. The transition between these phases are characterised by both rock contraction and expansion and thermal cycles show a hysteresis effect observed in the laboratory and the field. Snow cover controls the number of daily temperature changes, while topographic factors influencing insolation (e.g. aspect) controls the magnitude of temperature changes. Months-long slow crack opening occurred within a temperature range between -9 and -1°C suggested that ice segregation caused slow fracture opening reversed by ice relaxation. Depending on the dipping of shear planes, thermal changes on annual scale causes rock creeping that widen or shorten fracture aperture. Cycles of thermal- and ice-induced crack opening and closing can progressively weaken rockwalls and trigger rockfall. Climate change will shorten snow duration and increase temperature extremes, therefore, will affect the number and the magnitude of thermal changes and associated stresses. However, an earlier snowmelt in combination with temperature increase will decrease the occurrence of ice segregation and will shift the frost favouring temperature regime to higher altitudes. Therefore, climate change will change the frequency, magnitude and the location of thermal and ice-induced stresses and will change the spatial variation of rockfall in alpine environments in the future."

Specific Comments

Dummy Crackmeters. The use of the word "Dummy" should probably be changed to "Control". Dummy implies that the device does not provide any useful information. Regarding the devices themselves, they are not quite control crackmeters either, however, since they are still measuring rock deformation, just not across a fracture. Thus, whereas they provide some guidance for understanding the fracture measurements, there use should be put into context that they are better for understanding the nonfractured behaviour of the rock mass. Also, since the crackmeters were temperature corrected (L113), it was unclear how the controls were used for verification of the measured signals.

Thank you for this comment. I changed the wording from dummy to control crackmeter. The aim of the control crackmeters was to validate the findings of the laboratory tests. To clarify this, I added the information to the objectives at the end of the introduction: "Furthermore, I installed control crackmeters and rock temperature loggers on intact rocks at four rockwalls reaching from 2585 to 2935 m in elevation to validate laboratory-derived rock deformation behaviour and to model thermal stresses." and in the method section: "To validate rock deformation (RD) observed in the laboratory, one crackmeter was used as a control crackmeter and was fixed on intact bedrock without any cracks (Fig. 3)."

Thermal Shock. The term thermal shock is used to describe rapid deformation and fracture observed in several previous studies (L265), however my understanding is that those studies did not depend on rapid temperature increases to cause the deformation. Rather, thermal shock has been more accurately described by others such as Hall, especially in the context of Antarctic environments which might be applicable to this study. This could be a case of needing to be more clear as to what temporal range thermal shock applies to.

The reviewer is right and thermal shock is defined differently. Hall and Thorn review the process of thermal shock. They state that thermal stress is generated by sudden temperature changes that exceed the strength of material. The temperature change can be warming or cooling. The authors also

summarize different thresholds that depend on temperature changes per time and are all larger than 1°C min^{-1}. Therefore, I conclude that my observed rock deformation is not associated to thermal shock and more associated to temperature gradients between the rock surface and the rock interior. I omitted the term thermal shock and changed the text in the discussion to: "After stopping cooling and enhancing a natural warming of the rock samples, the (2) transition phase started (Fig. 5a-b). Some crackmeters experienced a sudden rock deformation due to rapid rock response to warming, while other crackmeters even on the same rock sample showed further rock contraction (Fig. S1-2). The contraction behaviour corresponded to decreasing RT5 cm, while RTT was already increasing as a response to warmer air temperature. Therefore, the transition phase is characterized by a temperature difference between rock surface (RTT) and rock depth (RT5cm), which is a result of the slow speed of heat conduction. While the rock surface (RTT) was warming and rock was expanding, the overall rock kinematics was still controlled by cooling of the rock interior and associated contraction."

Technical Corrections

L10-12. Suggest rewrite without the numbers (i.e., (1), (2), etc.). This reads awkwardly and the main points of the study are therefore not presented clearly.

Done.

L11. Change to ". . .kinematics of intact rock samples. . ."

I rewrote the text to: "In this study, I quantify thermal- and ice-induced rock and fracture kinematics and place these in the context of their role in producing rockfall and climate change."

L13. Change to ". . .2935 m in elevation."

Done.

L31. Change to "and amplify fracturing by thermo-hydro-mechanical. . ." The sentence requires a verb, so this fixes the issue.

Done.

L63. Remove numbers of main points and try summarizing in more typical sentence form.

Done.

L63. Change to "Furthermore, I installed. . ."

Done.

L126. The use of the C1, C2 terminology should be clarified as these are not shown in Fig. 2.

I changed the labelling of laboratory crackmeters to RD1 and RD2 in the text, which is consistent to Fig.2.

L161. This section should likely be placed in the Methods.

I followed the advice and incorporated the section into the method section:" To monitor fracture movement in the field, I installed three 0.4 m long Geokon Vibrating-Wire Crackmeters 4420-1-50 with resolution of 0.0125 mm and accuracy of 0.05 mm at RW-1 to RW-3 in 2016 (Fig. 3a-c). Instrumented rockwalls range from 2585 m (RW-3), 2672 m (RW-2) to 2935 m (RW-1) and are exposed in northwest (NW) to northeast (NE) direction (Fig. 1; Table 2). Rock strength of each rockwall was measured using a N-type Schmidthammer following Selby (1980, Table 3). At RW-1, a 3.5 m long, 1.9 m wide and 2.1 m high aplite block was monitored (Fig. 3a). A slickenslide on top of the block indicates former movement of a previously above-laying block. The monitored block slides on a 20 to 40° inclined shear plane (J3 in Fig. 3a) into the valley with an identical angle than the slickenslide. The block is separated by a 10 to 70 mm wide crack of joint set 1 (J1) from a second 2.5 m long and 2.6 m high block. At RW-2, three blocks were monitored which are incorporated in a heavily fractured rockwall consisting of amphibolite. All monitored cracks possess an aperture between 1 and 2 mm (Table 1) and are dipping at 50° out of the rockwall (J2), however, the blocks are buttressed by adjacent blocks and the talus slope (Fig. 3b). RW-3 consists of schistose quartz slate and blocks are 0.3 to 1.5 m wide (Fig. 3c). Blocks are separated by 81° inclined and 30 to 50 mm wide cracks (J2), which were monitored. The schist cleavage is dipping at 22° into the rockwall.

To identify effects of different exposition, three more crackmeters were installed at RW-S at 2723 m in 2017 (Fig. 3d). RW-S is heavily fractured, which results in the occurrence of a high number of joint sets (Fig. 3d). The monitored blocks dip with an angle of 41° degrees into the rockwall (H2) and crack aperture range from 7.5 to 20 mm at Crack-2 to 45 to 135 mm at Crack-1 (Table 2)."

Fig. 1. It would be helpful to point out that the red parallelogram in (d) is the area shown in (c).

I changed the figure caption and added one sentence: "The red parallelogram highlights the photo extend of (c)."

Fig. 4. The forward slash symbol should not be used in the y-axis label, as this appears to represent that rock temperature is being divided by rock top temperature. Better to use a comma to avoid confusion. In addition, consider spelling out some of the abbreviations so that consultation with the caption is not necessary. At a minimum, the rock types could be spelled out, and perhaps the y-axis labels.

AND

Fig. 5. The time frame over which the data is presented is not shown. This is needed to identify the hysteresis effect.

I followed the reviewer's advice and changed the "RT/RTT" to "RT, RTT" in all figures. I also added a time frame and arrow indicating warming and cooling to Figure 5 and Figure S2 in the supplementary information.

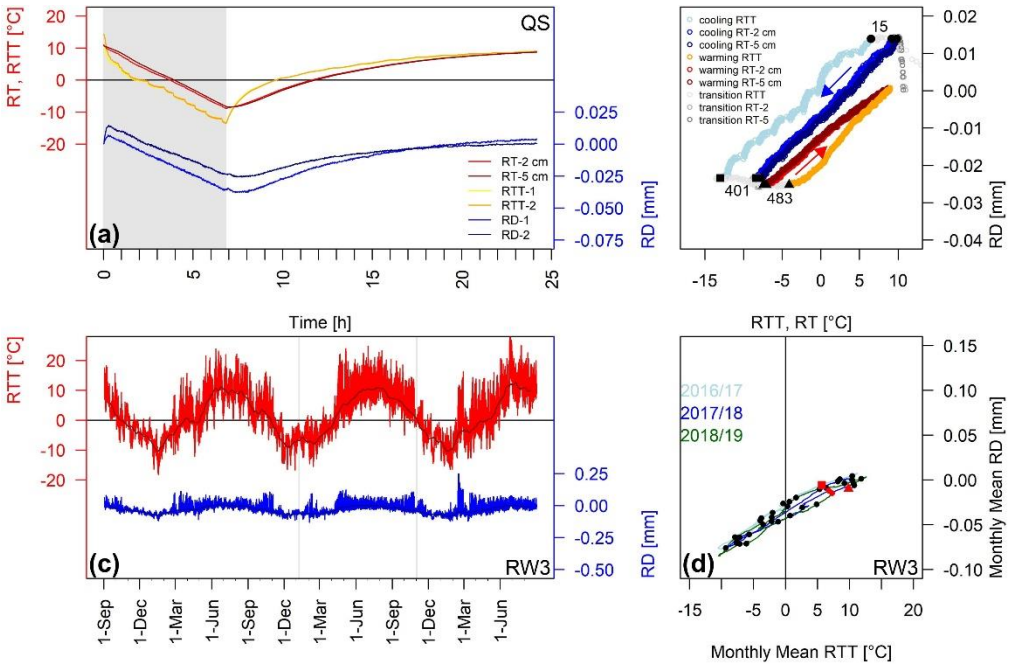

Figure 5: Laboratory crackmeter measurements of rock samples. (a) Rock-top temperature (RTT), rock temperature (RT) and rock deformation (RD) of crackmeter 1 and 2 plotted versus time for the schistose quartz slate sample (QS). (b) Rock deformation plotted versus rock-top temperature or rock temperature for crackmeter 2 of QS. Numbers indicate the timing of the beginning of the cooling period (black dot), end of the cooling period (black rectangle) and beginning of the warming period (black triangle). Arrows highlight the temporal trajectory of cooling (blue) and warming (red). Results of all laboratory measurements are shown in Fig. S1 and S2 in the supplementary information. Field measurements of the control crackmeter at RW3. (c) RTT (red line) and monthly mean RTT (dark red line), RD (blue line) and monthly mean RD (dark blue line) plotted versus time for the period from 1 September 2016 to 31 August 2019. Grey rectangles highlight the occurrence of snow cover. (d) Monthly mean rock deformation plotted versus monthly mean RTT. Red rectangles indicate start, black dots first day of a month, red dots the beginning of new measurement period and red triangles the end of measurements. Colour of graphs indicate data from 2016/17 (light blue), from 2017/18 (blue) and 2018/19 (green). For results of RW1 and RWS, see Fig. S3 in the supplementary information.

Anonymous Referee #2

While not being an expert of the type of research presented in this manuscript, I must say that the description of the methods, data and results looks report-like and seems to be very technical. For non-experts of fracture dynamics related to cooling-warming phases, and maybe also for experts, the research outline is quite tedious. The essential outcome of the laboratory and field tests thus appears to be almost hidden behind these technical descriptions.

Methods, data and results shall be described more concisely, highlighting more the added value of these parallel lab and field tests, for rock mechanics and related hazard understanding. .. that appears a bit as an appendant at the end of the conclusions. Therefore, I doubt that this paper as such would attract the attention of a wide readership - even though the scientific basis is of a high level.

I like to thank the reviewer for her/his comments. I can understand that my report-like, very technical writing style almost hide my findings. I completely revised the method, result and discussion section following the comments of Reviewer 1. The revised method section starts now with a section describing the laboratory measurements. I added information on mechanical and seismic rock properties that I use for a thermal stress model, I added to the manuscript:

"To understand controlling factors of rock kinematics, I conducted laboratory measurements on air-dryed rock samples in a freezing chamber. For this purpose, I collected three approximately 0.4 m long, 0.15 m wide and 0.2 m high rock samples without visible evidence of weathering from talus slopes below rockwalls with lithologies ranging from aplite (AP, RW-1), amphibolite (AM, RW-2) to schistose quartz slate (QS, RW-3; in Fig. 1d). I assume that the rock samples are representative for the rockwall. On each rock sample (Fig. 2), two crackmeters were installed at the top (RD1) and at one side of the sample (RD2) to monitor rock deformation (RD) and rock top temperature (RTT) in 1 min intervals. The two Geokon crackmeters 4420-3 measured RD and automatically correct thermal expansion of the instrument. After temperature correction, the resolution of RD is below 0.00075 mm with an accuracy below 0.003 mm, while RTT is measured with an accuracy of ±0.5°C. Two high-precision Greisinger thermistors connected to a Pt 100 temperature sensor (0.03°C accuracy) were used to monitor rock temperature in the center of the rock sample in 5 cm depth (RT_{5cm}) and in 2 cm depth (RT_{2cm}). To keep room temperature constant at low levels, the freezing chamber is located in a fridge that keeps the surrounding temperature at 8 to 10 °C. The freezing chamber itself consists of a custom-made Fryka cooler with a temperature-controlled (0.1°C accuracy) ventilation system to enable cooling of samples without thermal layering. The rock samples were cooled down from 10-14 °C to -8/9 °C RT_{2cm} in 7-9 h. Then, I stopped cooling and enhanced a "natural" warming for 15 to 17 h until 8 °C RT_{2cm} was reached. Based on the linear correlation, I derived the thermal expansion coefficient α:

$$\alpha = \frac{1}{L} * \frac{\Delta RD}{\Delta RT} \quad (1)$$

with L is crackmeter length, ΔRD is rock deformation change and ΔRT is rock temperature change.

Young modulus *E* and Poisson' ratio *υ* were derived using a Geotron ultrasonic generator USG40 in combination with Geotron preamplifier VV51 and 20 kHz sensors (Table 1). Seismic signals were recorded using a PICO oscilloscope and data analyzed using the software Geotron Lighthouse DW. Uniaxial compressive strength σ_u and tensile strength σ_t was measured (Table 1) in accordance to norms of the German Geotechnical Society by Mutschler (2004) and Lepique (2008). For a more detailed description of the seismic and mechanical tests see Draebing and Krautblatter (2019)."

Subsequently, I describe my field measurements. Following the recommendation of Reviewer 1, I included the fracture information formerly presented in 4.2.2. into this section. I will validate my thermal stress model using Schmidt hammer measurements, I shortly introduced in one sentence in this section: "To monitor fracture movement in the field, I installed three 0.4 m long Geokon Vibrating-Wire Crackmeters 4420-1-50 with resolution of 0.0125 mm and accuracy of 0.05 mm at RW-1 to RW-3 in 2016 (Fig. 3a-c). Instrumented rockwalls range from 2585 m (RW-3), 2672 m (RW-2) to 2935 m (RW-1) and are exposed in northwest (NW) to northeast (NE) direction (Fig. 1; Table 2). Rock strength of each rockwall was measured using a N-type Schmidt hammer following Selby (1980, Table 3). At RW-1, a 3.5 m long, 1.9 m wide and 2.1 m high aplite block was monitored (Fig. 3a). A slickenslide on top of the block indicates former movement of a previously above-laying block. The monitored block slides on a 20 to 40° inclined shear plane (J3 in Fig. 3a) into the valley with an identical angle than the slickenslide. The block is separated by a 10 to 70 mm wide crack of joint set 1 (J1) from a second 2.5 m long and 2.6 m high block. At RW-2, three blocks were monitored which are incorporated in a heavily fractured rockwall consisting of amphibolite. All monitored cracks possess an aperture between 1 and 2 mm (Table 1) and are dipping at 50° out of the rockwall (J2), however, the blocks are buttressed by adjacent blocks and the talus slope (Fig. 3b). RW-3 consists of schistose quartz slate and blocks are 0.3 to 1.5 m wide (Fig. 3c). Blocks are separated by 81° inclined and 30 to 50 mm wide cracks (J2), which were monitored. The schist cleavage is dipping at 22° into the rockwall.

To identify effects of different exposition, three more crackmeters were installed at RW-S at 2723 m in 2017 (Fig. 3d). RW-S is heavily fractured, which results in the occurrence of a high number of joint sets (Fig. 3d). The monitored blocks dip with an angle of 41° degrees into the rockwall (H2) and crack aperture range from 7.5 to 20 mm at Crack-2 to 45 to 135 mm at Crack-1 (Table 2).

All crackmeters were fixed by groutable anchors and half tubes protected the devices from snow load (Draebing et al., 2017a; Draebing et al., 2017b). At each rockwall, two crackmeters spanned cracks to monitor crack deformation (CD) and crack-top temperature (CTT). To validate rock deformation (RD) observed in the laboratory, one crackmeter was used as a control crackmeter and was fixed on intact bedrock without any cracks (Fig. 3). Due to snow load damage or technical failures, crackmeters had a different life span and the control crackmeter at RW-2 failed to record data completely. A 4-Channel Geokon data logger Lc2x4 recorded all data at each rockwall in 3h intervals between 1 September 2016 and mid-August 2017 and in 1h intervals from mid-August 2017 to 31 August 2019. Crackmeter data were temperature-corrected, residual uncertainty quantified and the existence of snow cover was deviated using daily standard deviation of CTT or RTT following the technique by Schmid et al. (2012). To analyse the overall fracture movement pattern (Bakun-Mazor et al., 2013), a monthly moving average of CD, RD, CTT and RTT was calculated. The thermal expansion coefficient of the control crackmeters was calculated based in Eq. 1."

In the last part of the method section, I shortly introduced the meteo data, rock temperature data and the thermal stress model:" Air temperature and snow depth data was derived from the meteo station Oberer Stelligletscher (2910 m) located 2.5 km SE of the research area in the Matter Valley (MeteoSwiss, 2019a). Probably due to snow cover above 3.5 m, there is a data gap from mid-January to end of February 2018. The temperature data gap was filled using air temperature adapted from near-by meteo station Grächen at 1605 m (MeteoSwiss, 2019b) by applying a linear correlation (r^2= 0.85). To monitor rock surface temperature (RST), I installed four Maxim iButton DS1922 L temperature loggers with a nominal accuracy of ±0.5 °C in 10 cm deep boreholes following the measurement method by previous studies (e.g. Draebing et al., 2017a; Haberkorn et al., 2015). The loggers recorded RST in 3h intervals between 1 September 2016 and 31 August 2019 (RW1-3) or between 1 September 2017 and 31 August 2019 (RWS), respectively. Due to the logger location in 10 cm depth, I determined snow cover duration using the uniform standard deviation threshold of <0.5 K for positive and negative RST in accordance to Haberkorn et al. (2015). I calculated daily rock temperature warming and cooling cycles ΔRT and applied the equation from Anderson and Anderson (2012) to model thermal stress σ_{th}:

$$\sigma_{th} = \frac{\alpha\, E\, \Delta RT}{(1-\upsilon)}. \qquad (2)$$"

I shortened the result section by 40 % and focused on the presentation of the main findings that support my objectives. I first present the air and rock temperature because this information is necessary to understand the climatic context. I incorporated a new Figure that presents the meteo data, rock surface data and the thermal stress model results:

"At the meteo station at 2910 m, mean annual air temperature (MAAT) ranged from -0.6 °C in 2016/17, to -1.0 °C in 2017/18 and -1.1°C in 2018/19. Daily air temperatures fluctuated between -20 °C and 12 °C (Fig. 4a). After a short period of snow cover with snow depths up to 75 cm between November and December 2016, a second period of snow cover with snow depths up to 150 cm started in mid-January 2017 and lasted until mid-July 2017. Snow onset in the following year was delayed and started at the end of December 2017. Snow depths reached more than 350 cm and lasted until mid-August 2018. After approximately 2 months without snow, snow cover period started at the end of October 2018 and lasted until the end of July 2019 with snow depths up to 250 cm. Cooling periods lasted from mid-

August to mid- January 2017, April 2018 or mid-February 2019 and mean monthly air temperature dropped to -12° C. The warming period lasted 4.5 to 7 months and reached a mean monthly air temperature of 6°C in mid-August.

Rock surface temperatures (RST) followed the annual and daily oscillation of air temperatures. At annual scale, RST of north-exposed rockwalls ranged from -12.9 °C up to 13.4 °C for RW1, -5.6 °C up to 17.6 °C for RW2 and -7.0 °C up to 13.9 °C for RW3 (Fig. 4b-d). In contrast, the south-exposed logger at RWS recorded higher RST variations between -12 °C and 32 °C (Fig. 4e). At daily scale, the north-facing loggers measured small daily temperature variations up to 4 °C, whereas the south-exposed logger recorded variations up to 16.5 °C. Snow cover attenuated daily temperature oscillations with expected high deviation between north- and south-exposed rockwalls. At north-facing rockwalls, snow cover onset was between October and November and lasted between 220 days and 251 days per year with only minor differences between RW1 to RW3 and individual years (Fig. 4b-d, Table 3). In contrast, snow onset was delayed to mid- February 2018 or snow cover was only sporadic in 2019, therefore, snow cover duration was reduced to 5to 80 days (Fig. 4e).”

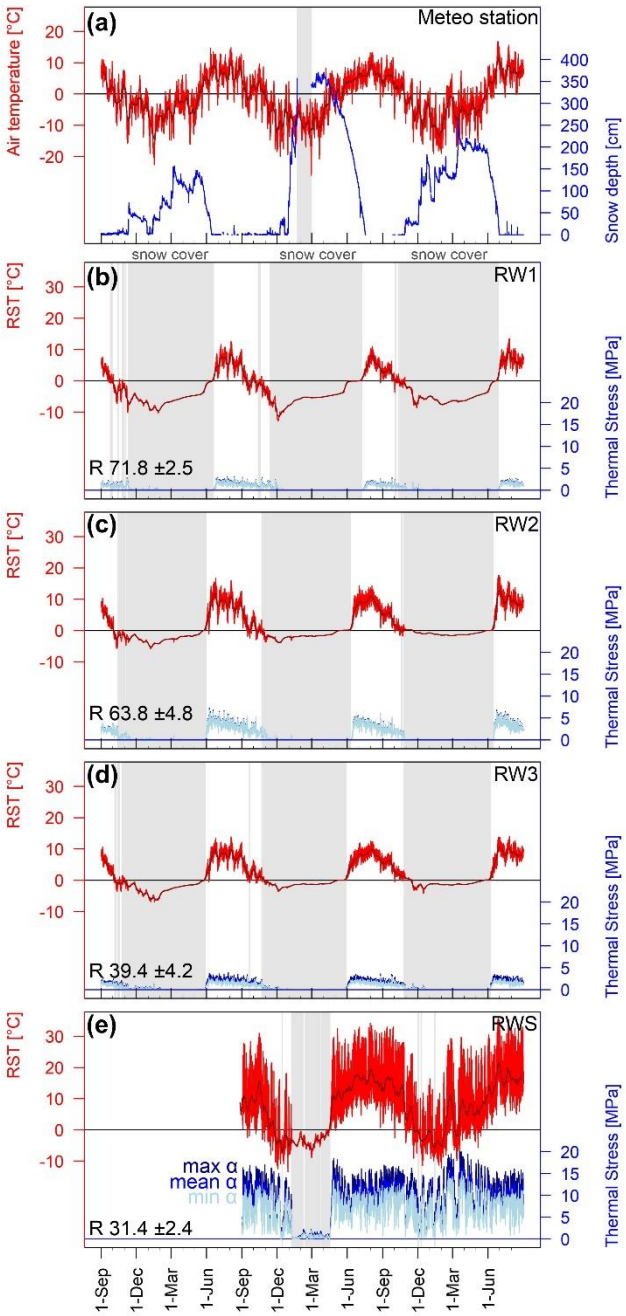

Figure 4: (a) Air temperature and snow depth from meteo station Oberer Stelligletscher plotted for the period from September 2016 to August 2019. Rock surface temperatures (red lines) and mean 10-day RST (dark red line) recorded by iButtons installed at (b) RW1, (c) RW2, (d) RW3 and (e) RWS. Thermal stress was modelled using minimum α (light blue lines), mean α (blue lines) and maximum α (dark blue lines) Grey rectangles highlight the data gap filled with modelled air temperatures in (a) and snow cover (b-e). Numbers represent measured Schmidt hammer rebound values R.

Then I present the laboratory tests and validate the observed pattern using the control crackmeters (former dummies). I shortened the description and focus on my main findings: the warming and cooling cycles with different thermal expansion coefficients. I merged Figures 4 and 5 into a new Figure 5 by presenting only the information of the schistose quartz slate sample and RW3. All other subfigures I moved to the supporting information. I show that my control crackmeters show identical behaviour as my lab data. Furthermore, I use the measured thermal expansion coefficients of my lab tests in combination with rock temperature data to model the thermal stress regime. My data clearly shows

that the occurrence of thermal stresses is controlled by snow cover while the magnitude is controlled by topographic controlled insolation (e.g. aspect). I changed the second section of the results to:

"Directly after the start of cooling, several crackmeters revealed a rock expansion, which lasted for a few minutes (initial transition phase; Fig. 5a and Fig. S1c, e-f). Rock samples were cooled down to a RTT between -13.2 °C and -18.4 °C and all crackmeters experienced a negative RD (Fig. 5a-b, Fig. S1-2). Rock temperature in 2 to 5 cm depth was up to 5 to 7 °C higher than RTT during the cooling phase (Fig. 5 and S1-2). Based on $RT_{5\,cm}$ measurements using Eq. (1), thermal coefficient ranged from 5.8 ±0.0 10^{-6} $°C^{-1}$ for AM (r^2=1) to 7.3 ±0.2 10^{-6} $°C^{-1}$ (r^2=0.99) for AP and 7.3 ±0.5 10^{-6} $°C^{-1}$ (r^2=1) for QS during cooling. Nine to 23 min after stopping cooling, several crackmeters at all rock samples (AP RD_2, AM RD_2, QS RD_1 and RD_2) experienced a sudden rock deformation ranging from +0.004 mm to +0.0135 mm (transition phase; Fig. 4b, Fig, S2). Despite an increase of RTT from -7.3 to -5 °C, the QS sample and AP RD_1 and AM RD_1 showed a further rock contraction between -0.0016 mm and -0.0032 mm. The closing behaviour corresponded to the decrease of $RT_{5\,cm}$ from -8.2 °C to -9.3 (Fig. 4b). Subsequent warming up to 7.7 or 8 °C RTT resulted in rock expansion (warming phase, Fig. 5a-b and S1-2). This warming phase induced a thermal expansion that corresponds to a thermal expansion coefficient of 7.5 ±0.4 10^{-6} $°C^{-1}$ (r^2=1) for AP, 7.0 ±0.2 10^{-6} $°C^{-1}$ (r^2=1) for AM and 7.1 ±1.7 10^{-6} $°C^{-1}$ (r^2=0.99) for QS. All samples showed a hysteresis effect during warming and cooling cycles (Fig. 4b, Fig. S2), which was amplified using RTT and decreased with further rock temperature depth from $RT_{2\,cm}$ to $RT_{5\,cm}$.
Control crackmeters were installed in the field to validate laboratory-observed rock deformation. RTT fluctuated between -15 °C and 10 °C at RW1 in 2017/18, between -20 °C and 25 °C at RW3 from 2016 to 2019 and from -15 °C to 25 °C at RWS from 2017 to 2019 (Fig. 5c, Fig. S3). All control crackmeters showed small daily fluctuations of rock deformation that were even reduced when snow cover occurred. Similar to laboratory experiments, control crackmeters recorded cyclic rock expansion during warming and contrary rock contraction during cooling periods (Fig. 5 d, Fig. S3). The thermal expansion coefficients for cooling and warming based on monthly mean RD and RTT was 6.5 10^{-6} $°C^{-1}$ for RW1 (r^2 = 0.43), 9.4 10^{-6} $°C^{-1}$ for RW3 (r^2 = 0.94) and 9.0 10^{-6} $°C^{-1}$ for RWS (r^2 = 0.9). All control crackmeters showed a hysteresis effect, which was amplified at RW1.

Applying laboratory derived thermal expansion coefficients (Table 1) for warming and cooling to Eq. (2) provides the daily thermal stresses within a rockwall. Daily thermal stresses reflected RST and were increased during snow-free periods in summer and decreased or absent during snow cover periods. Maximum stresses reached up to 2.9-3.0 MPa at RW1, 6.8-7.2 MPa at RW2, 3.1-3.9 MPA at RW3 and 15.4-20.1 MPa at RWS (Fig. 4b-e)."

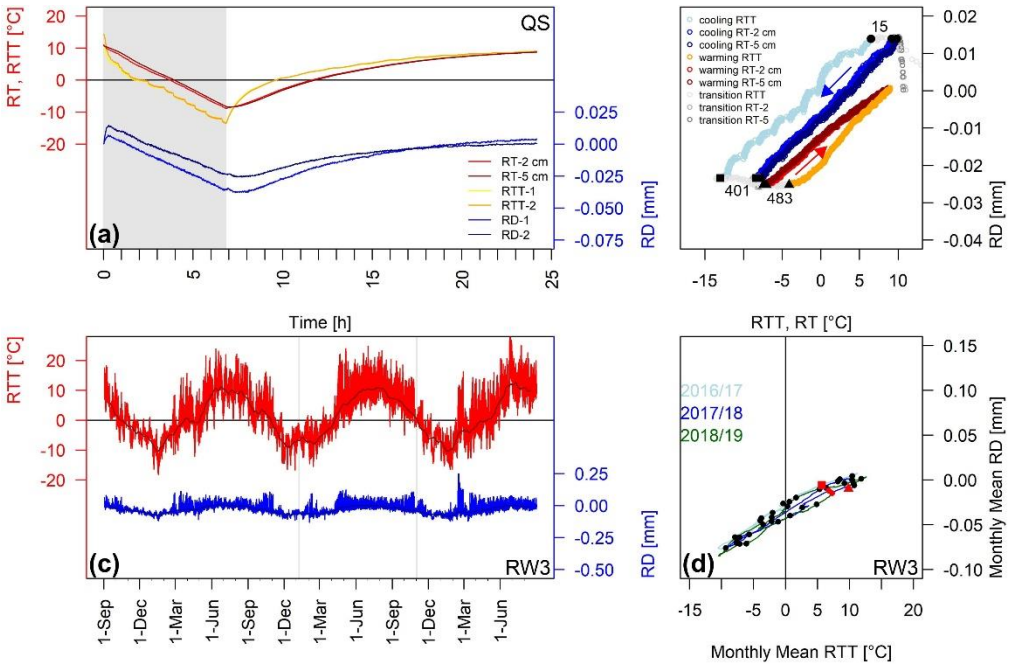

Figure 5: Laboratory crackmeter measurements of rock samples. (a) Rock-top temperature (RTT), rock temperature (RT) and rock deformation (RD) of crackmeter 1 and 2 plotted versus time for the schistose quartz slate sample (QS). (b) Rock deformation plotted versus rock-top temperature or rock temperature for crackmeter 2 of QS. Numbers indicate the timing of the beginning of the cooling period (black dot), end of the cooling period (black rectangle) and beginning of the warming period (black triangle). Arrows highlight the temporal trajectory of cooling (blue) and warming (red). Results of all laboratory measurements are shown in Fig. S1 and S2 in the supplementary information. Field measurements of the control crackmeter at RW3. (c) RTT (red line) and monthly mean RTT (dark red line), RD (blue line) and monthly mean RD (dark blue line) plotted versus time for the period from 1 September 2016 to 31 August 2019. Grey rectangles highlight the occurrence of snow cover. (d) Monthly mean rock deformation plotted versus monthly mean RTT. Red rectangles indicate start, black dots first day of a month, red dots the beginning of new measurement period and red triangles the end of measurements. Colour of graphs indicate data from 2016/17 (light blue), from 2017/18 (blue) and 2018/19 (green). For results of RW1 and RWS, see Fig. S3 in the supplementary information.

I shortened the results section on fracture kinematic by 50 % and focused concisely on the patterns. I identified four phases that I highlighted in Figure 6:

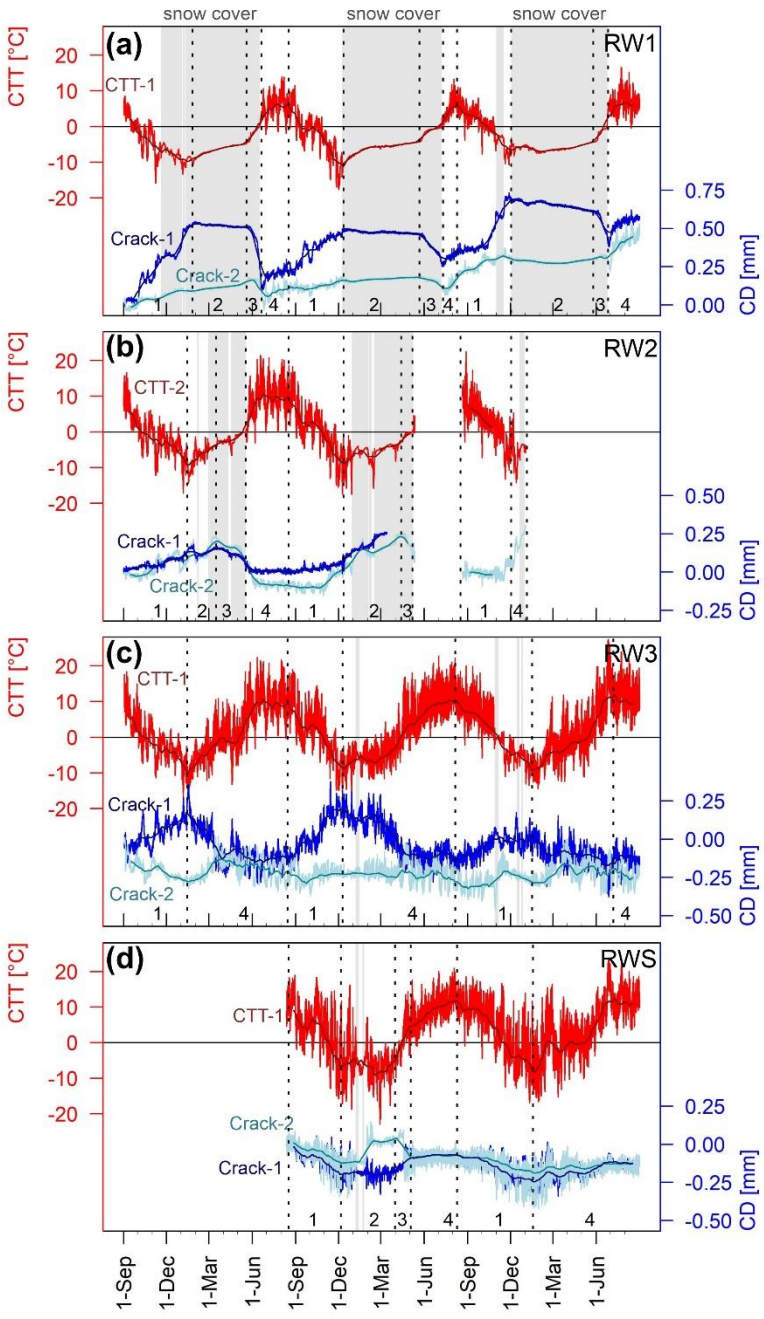

Figure 6: Crack-top temperature, monthly mean crack-top temperature, crack deformation and monthly mean crack deformation for the crackmeters at (a) RW1, (b) RW2, (c) RW3 and (d) RWS for the period 1 September 2016 to 31 August 2019. Grey rectangles highlight the snow cover period, while numbers indicate the interpreted phases (see Table 4).

I added a new Table 4 that summarizes the kinematic patterns of these phases as well as presents annual and overall deformation:

Table 4: Quantified rock fracture kinematic phases, annual and overall crack deformation in mm. Crack deformation (CD) is differentiated in crack closing (-), crack opening (+) and no CD (±).

Phases/	RW1		RW2		RW3		RWS	
Cumulative crack deformation	Crack-1	Crack-2	Crack-1	Crack-2	Crack-1	Crack-2	Crack-1	Crack-2
Phase 1: cooling period								
2016-17	+0.53	+0.09	+0.13	+0.09	+0.17	-0.28		
2017-18	+0.22	+0.04			+0.33	+0.01	-0.20	-0.12
2018-19	+0.32	+0.08			+0.15	±0.00	-0.18	-0.10
Phase 2								
2017	-0.05	+0.07	+0.02	+0.11				
2018	+0.02	+0.03						+0.16
2019	-0.08	-0.01						
Phase 3								
2017	-0.31	-0.10	-0.15	-0.29				
2018	-0.18	-0.07						-0.13
2019	-0.12	+0.03						
Phase 4: warming period								
2017	+0.07	+0.05			-0.31	+0.04		
2018	+0.06	+0.12			-0.33	-0.05	+0.14	±0.00
2019	+0.06	+0.11			-0.13	-0.04	+0.13	+0.08
cumulative annual CD								
2016/17	+0.24	+0.11	±0.00	-0.10	-0.09	-0.24		
2017/18	+0.12	+0.12			-0.02	-0.08	-0.06	-0.09
2018/19	+0.20	+0.22			-0.13	+0.07	-0.03	-0.04
overall CD	***+0.56***	***+0.45***			***-0.24***	***-0.25***	***-0.09***	***-0.13***

I restructured my result section and focussed on the identified phases:

"Crackmeters showed a decrease of snow duration with decreasing elevation. Crackmeters at RW1 located at 2935 m experienced 192 to 223 days of snow cover per year (Fig. 6). The number of snow-covered days was reduced to 69 and 73 days in 2016/17 at RW2 at 2672 m. Snow load damaged the equipment in the following years, which resulted in a data gap and incomplete measurement of snow cover duration. RW-3 at 2585 m showed between zero and nine days of snow cover and snow cover was limited to two days at Crack-2 in 2017/18 at the south-facing rockwall RWS.

All crackmeters experienced a cooling period (Phase 1 in Fig. 6) that ranged from September until mid-December to Mid-February. At RW1, the onset of snow cover controlled the end of the cooling period, only in 2016/17 cooling continued under snow cover. The cooling period was characterized by a crack opening (Table 4), which was between 0.22 and 0.53 mm at Crack-1 and between 0.04 and 0.09 mm at Crack-2 at RW1. At RW2, cracks opened between 0.09 mm at Crack-2 and 0.13 mm at Crack-1, while Crack-1 at RW3 revealed a crack opening between 0.15 and 0.33 mm. In contrast, Crack-2 at RW3 experienced a diverse crack deformation ranging from crack closing between 0.28 mm to 0.01 mm crack opening. At RWS, the cooling period was characterized by crack closing between 0.18 and 0.20 mm at Crack-1 and between 0.1 and 0.12 mm at Crack-2.

At RW1 and RW2, crackmeters experienced a slow warming below snow cover (Phase 2 in Fig. 6), which resulted in either crack opening or crack closing (Table 4). Crackmeters at RW1 experienced a crack deformation ranging from closing of 0.08 mm to crack opening of 0.07 mm. At RW2, cracks experienced a crack opening between 0.02 and 0.11 mm. At RWS, snow cover was absent during warming, however, Crack-2 experienced an opening of 0.16 mm, which was reversed by 0.13 mm during enhanced warming in 2017. RW1 and RW2 showed a period of predominantly crack closing during enhanced warming until snow cover completely melted (Phase 3 in Fig. 6). Crack-1 at RW1 experienced between 0.12 to 0.31 mm crack closing, while Crack-2 showed a diverse crack deformation ranging between 0.03 mm opening and 0.10 mm closing. At RW2, the crackmeters revealed crack closing between 0.15 and 0.29 mm.

All crackmeters experienced a warming period (Phase 4 in Fig. 6), which is characterized by both crack closing and crack opening (Table 4). At RW1, crackmeters revealed a crack opening between 0.05 and 0.12 mm. In contrast, RW3 showed a crack closing between 0.13 and 0.33 mm at Crack-1 and a crack deformation behaviour ranging from 0.07 crack opening to 0.24 mm crack closing at Crack-2. At RWS, the warming period is associated with crack opening between 0.00 and 0.14 mm. In the 3-year period, RW1 experienced a crack opening between 0.45 and 0.51 mm. In contrast, RW3 showed an overall crack closing between 0.24 and 0.25 mm. Data at RW2 was limited to 2016/17 and cracks experienced no change or 0.1 mm closing. RWS was characterized by crack closing in each year with a cumulative closing between 0.03 and 0.09 mm.

On a daily scale, cooling resulted in crack opening due to contraction of two rock blocks and warming in crack closing due to expansion of two rocks (Fig. 8). The peak of opening and closing between individual crackmeters can be different. Crackmeters at RW1 experienced daily CTT fluctuations in the range below 10°C and daily CD below 0.1 mm (Fig. 9) during snow-free periods. The fluctuations were increased up to 16°C and 0.11 mm at RW2, 23 °C and 0.26 mm at RW3 as well as 21°C and 0.32 mm at RW-S.“

I completely revised the discussion section. I omitted the repetitive description of results and focussed more on my identified patterns. Following the recommendations of Reviewer 1, I structured the discussion along Figure 11 (now Fig. 10). In the first section, I focus on “5.1 Cyclic thermal rock deformation”. My major findings disused in this section are:

My laboratory data show that warming and cooling on sample scale shows a trajectory with different thermal expansion coefficients and a hysteresis effect. My data can be used to drive a thermal stress model, as added to the revised manuscript. Thermal stresses can develop that can concentrate at fracture and widen these fractures. **My control crackmeters (former dummies) demonstrate that identical trajectories can be observed on annual scale**. I revised the first discussion section to: “Cyclic thermal stresses can result in thermal fatigue that breakdown rock and is an important component of mechanical weathering. In my laboratory tests, I can differentiate thermal cycles into three phases: (1) cooling phase, (2) transition phase, (3) warming phase. The (1) cooling phase was characterized by rock contraction with thermal coefficients α (Table 1), which are in the order of previous thermal expansion coefficients for quartz minerals (Siegesmund et al., 2008) or rock samples (Ruedrich et al., 2011; Skinner, 1966). After stopping cooling and enhancing a natural warming of the rock samples, the (2) transition phase started (Fig. 5a-b). Some crackmeters experienced a sudden rock deformation due to rapid rock response to warming, while other crackmeters even on the same rock sample showed further rock contraction (Fig. S1-2). The contraction behaviour corresponded to decreasing $RT_{5\ cm}$, while RTT was already increasing as a response to warmer air temperature. Therefore, the transition phase is characterized by a temperature difference between rock surface (RTT) and rock depth (RT_{5cm}),

which is a result of the slow speed of heat conduction. While the rock surface (RTT) was warming and rock was expanding, the overall rock kinematics was still controlled by cooling of the rock interior and associated contraction. The (3) warming phase was characterized by rock expansion (Fig. 4 and 5) with thermal expansion coefficients that are slightly different from the cooling (Table 1). Therefore, thermal cycles showed a hysteresis effect, which was previously observed on other lithologies (Ruedrich et al., 2011).

The control crackmeters demonstrated that snow cover controls the occurrence of daily temperature cycles, and associated rock expansion during warming and contrary rock contraction during cooling. Daily temperature changes affected the upper 0.21 to 0.42 m assuming a 12 h temperature cycle and a thermal diffusivity between 1 and 2 mm s^{-2} typical for metamorphic rocks (Vosteen and Schellschmidt, 2003; Cermák and Rybach, 1982). These rock depths correspond to daily temperature cycles in rockwalls observed in previous studies (Gunzburger and Merrien-Soukatchoff, 2011; Anderson, 1998). On annual scale, thermal changes affected 4 to 8 m and, therefore, the entire instrumented rock blocks assuming a half-year cycle and thermal diffusivities typical for metamorphic rocks. Rock temperature boreholes in the Alps suggest heat propagation to similar depths (Phillips et al., 2016a; PERMOS, 2019). Control crackmeters revealed identical phases of thermal-induced rock deformation as laboratory measurements including hysteresis effects. The hysteresis effect was amplified at RW-1, where rock blocks are between 2 and 4 times larger than rock blocks at the other rockwalls (Fig. 3). A larger rock block size results in a longer heat transfer by conduction and increases the transition phase, therefore, I interpret the increase of the hysteresis effect as a result from block size and an effect of scale. The observed differential thermal expansion in combination with different response during transition phase results in mechanical stresses able to breakdown rock that will be discussed in Chapter 5.3."

In the second part of the discussion section, I focus on the identified fracture kinematic patterns. My major findings are: **On daily scale, my data showed thermal-induced crack opening and closing. The occurrence is controlled by snow and the magnitude by insolation.** Furthermore my data suggest **the occurrence of slow ice-induced fracture opening that takes place in a temperature regime between -9 and -1° C very similar to the frost cracking window on seasonal scale**. Ice-induced fracture opening is assumed to be a preparing factor and also a trigger of rockfall, however, this process was rarely observed and only one study previously quantified this process. **On annual scale, my data demonstrated an irreversible rock movement due to rock creep**. Several field studies suggested that blocks can creep and that this creep can be irreversible. Laboratory studies confirmed this process, up to my knowledge this process was not observed or quantified before. I changed the section on fracture kinematics to: "In overhanging steep rock cliffs, thermal stresses can propagate fractures and trigger rockfall (Collins and Stock, 2016; Stock et al., 2012). Exfoliation joints warm differentially (Guerin et al., 2019) and thermal bowing results in fracture propagation parallel to the rockwall (Collins and Stock, 2016). In fractured rock, daily and annual thermal cycles result in rock contraction with fracture widening during cooling and rock expansion during warming with fracture closing (Fig. 11b; Cooper and Simmons, 1977; Draebing et al., 2017b). My data showed that crack opening and closing occurred on a daily scale (Fig. 8). The magnitude of this crack deformation depends on the magnitude of temperature change and was increased at RWS and RW3, which experienced much higher daily temperature changes (Fig. 9). The data demonstrated that the number of daily temperature changes per year (Fig. 9 and Fig. S5) is controlled by the duration of snow cover. Snow cover insulates the ground (Zhang, 2005) and decreases daily thermal changes (Fig. 10; Luetschg and Haeberli, 2005; Draebing et al., 2017b), therefore, rockwalls at lower elevations (e.g. RW3) or south-exposed rockwalls

(e.g. RWS) experienced a shorter snow cover duration (Table 2) and a higher frequency of thermal cycles than higher-elevated rockwalls with longer snow cover (e.g. RW2-3).

On seasonal scale, several crackmeters experienced a slow crack opening during negative CTT that suggest the influence of ice (Fig. 11c). Matsuoka (2001, 2008) observed rapid crack opening during freeze-thaw cycles in spring or autumn that suggest volumetric expansion as the trigger of crack opening. In contrast, I observed a slow crack opening lasting between 1.5 to 2 months at RW2 in 2017 (Fig. 6b and Fig. 7c-d), 3 to 3.5 months at Crack-2 at RWS in 2018 (Fig. 6d and Fig. 7h), and 5 to 5.5 months at Crack-2 at RW1 in 2017 and 2019 (Fig. 6a and Fig. 7b). The opening occurred in a CTT range between -5 to -3.3°C at RW2, between -8 and -3.6°C at RWS and -9 to -1°C at RW1. These temperature ranges are within the frost cracking window from -8 to -3 °C suggested by Anderson (1998) or in the range of laboratory observed frost cracking windows of aplite, amphibolite and schist quartz slate (Draebing and Krautblatter, 2019). The temporal trajectories of the affected cracks showed that crack opening occurred during warming within the negative temperature range (Fig. 7b-d. h), therefore, a purely thermal response of the rock would result in rock expansion and crack closing. In addition, a transition phase as observed in the laboratory or at control crackmeters can be excluded, thus, the transition phase is associated with temperature changes from warming to cooling or reverse, which were absent during these crack opening phases. Therefore, I interpret the observed crack opening as a result of ice segregation and subsequent closing because of ice relaxation. Cracks can infill with ice by refreezing of meltwater, ice infill growth slowly with time by cryosuction (Weber et al., 2018; Draebing et al., 2017b) and build up ice pressure and stresses in a subcritical range (Draebing and Krautblatter, 2019), which induce slow fracture opening (Draebing and Krautblatter, 2019; Draebing et al., 2017b).

On annual scale, thermal-induced crack opening and closing can be reinforced by cryogenic processes (Hasler et al., 2012), can propagate fractures (Ishikawa et al., 2004) and can result in irreversible rock movement (Weber et al., 2017). Previous studies focussed on toppling rock blocks (Ishikawa et al., 2004) or provided no information on the failure type (Hasler et al., 2012; Weber et al., 2017). Due to the tectonic setting, the observed blocks are located on a shear plane dipping out of the slope (RW1-2, Fig.3 a) or dipping into the slope (RW3, RWS; Fig. 3b-d). Gunzburger et al. (2005) observed daily non-permanent block movement and suggested that thermal changes can induce rock creep along shear planes. On non-buttressed blocks located on shear planes dipping out of the slope (RW1), crackmeters recorded annual and overall crack opening indicating that the lower located block in Figure 3 a is creeping slope downwards with an annual rate of 0.11 to 0.24 mm a^{-1} (Table 4). The majority of the creeping occurred during the cooling phase (Phase 1 in Fig. 6a), which was characterized by 0.22 to 0.53 mm opening of Crack-1 at RW1. This opening was slightly reversed at Crack-1 and extended at Crack-2 by ice segregation during phase 2. In Phase 3, the closing pattern reversed most of the previous crack opening. The warming phase 4 induced a crack opening, which is contrary to expected crack closing. Bakun-Mazor et al. (2020) identified thermally-induced wedging as a cause of crack opening during warming. The rock contracts during cooling and a wedge within the fracture sinks into the cooling-induced gap and causes a crack opening during warming induced thermal expansion. A wedge was not visible at Crack-1 and the annual opening exceed the crack opening during the warming phase 4. Therefore, I interpret the crack opening as irreversible thermal-induced block movement.

In contrast to RW1, all other block are located on shear planes dipping into the rockwall or buttressed by other blocks (Fig. 3b-d). The cooling phase resulted in crack opening at RW2 and Crack-1 at RW3 and the opening was reversed during the warming phase 4 resulting in an irreversible annual (RW2-3) and overall closing (RW3). Crack closing at Crack-2 at RW3 and RWS occurred during the cooling period and was not completely reversed during the warming period resulting in an annual and overall crack

closing (Table 4). In summary, thermal induced crack deformation caused an irreversible block movement along the shear plane into the rockwall (Fig. 11e)."

In the third part of the discussion, I focus on the climatic perspective of the observed rock and fracture patterns, link climate to rockfall and put these patterns in the context of climate change. Thermal changes cause thermal stress that can progressively crack rocks or widen existing fractures. I provide a quantitative measure for the stress acting on intact rocks. **My data demonstrated that snow cover controls the occurrence of thermal changes and stresses**. Snow cover duration depends on elevation and **climate change will reduce the snow cover period**, therefore, **more thermal stresses will occur**. In addition climatic extremes will occur more frequent, which can **increase the thermal stress magnitude**. "Thermal changes are an important climatic factor inducing stresses responsible for mechanical weathering (Eppes and Keanini, 2017). Thermal stresses cause subcritical cracking (Eppes et al., 2016) and propagate fractures (Eppes et al., 2010; Eppes and Keanini, 2017). In alpine rockwalls, thermal changes result in deformation of rocks (Guerin et al., 2020; Collins and Stock, 2016) and induced stresses can decrease the strength of stability-relevant rock bridges (Guerin et al., 2019) and can trigger rockfall (Stock et al., 2012; Collins and Stock, 2016). Applying the observed thermal coefficients and recorded RST in 10 cm depth to the thermal stress model by Anderson and Anderson (2012) demonstrated that thermal stresses occurred during snow-free periods and during periods of thin snow cover before snow achieved sufficient height to insulate the rock surface (Phillips, 2000; Luetschg and Haeberli, 2005). Modelled thermal stresses represent maximum values, thus, the equation (2) assumes isotropic material and an equal volumetric expansion in every direction. Occurring rock types possess cracks and schist planes, which results in anisotropy ranging between 0.05 for amphibolite, 0.06 for aplite and 0.55 for schistose quartz slate (Draebing and Krautblatter, 2019). Therefore, modelled stresses for schistose quartz slate are potentially overestimated. Stresses will concentrate at crack tips and widen cracks (Eppes and Keanini, 2017), however, stress calculation requires knowledge on crack geometry which is not available. The applied model provides a quantitative measure of stress levels and demonstrates that stresses occurring at RW1-3 are below tensile strengths and compressive strengths of in-situ rock (Table 1). Thermal stresses are not exceeding rock strength and are subcritical in sensu Eppes and Keanini (2017), however, the cyclicity of thermal stresses progressively weakens rock (Eppes et al., 2016). Schmidt hammer values showed high values between 63 ±4.8 and 71.8 ±2.5 for RW1-2, which consist of high-strength aplite and amphibolite (Table 1), therefore, these values suggest minor weathering near the surface. In contrast, rockwalls with schistose quartz slate revealed lower rebound values with RWS had lower (31.4 ±2.4) values than RW3 (39.4 ±4.2). This could be a result of higher modelled thermal stresses at RWS compared to RW3 (Fig. 4). However, thermal processes are not acting isolated and other weathering processes including mechanical, chemical and biological weathering can be responsible for the observed decrease in rock strength (Viles, 2013b; Eppes and Keanini, 2017). As soon cracks are existent, daily thermal changes induce fracture kinematics that can widen cracks (Fig. 10b). My data demonstrated that snow cover controls the number of daily crack deformation (Fig. 8 and Fig. S5). According to Bender et al. (2020), the changes of snow duration is elevation dependent and locations in Valais above to 2500 m will experience a shortening of the snow season of approximately 10 % by 2035, 17 % by 2060 and 25 % by 2085. Temperature extremes and variability (Schär et al., 2004; Gobiet et al., 2014) will increase in the future. Therefore, the number and the magnitude of thermal stresses will increase in the future, which could be amplified if climate becomes wetter (Eppes et al., 2020). Consequently, thermal stresses will play a more important role in preparing and triggering rockfall in the future."

Cryogenic processes are controlled by the thermal regime (e.g. frost cracking window). The process progressively weakens rock. **Climate change will cause earlier snowmelt, which shortens the period of the frost cracking window**. In addition, climate change induced warming will **shift the altitude of the frost cracking window**. Therefore, rockfall patterns related to frost cracking will change. "Cryogenic processes can cause fracture movement (Draebing et al., 2017b) and produces subcritical stresses that are below tensile strengths of rocks (Draebing and Krautblatter, 2019). These stresses occur in a wide temperature range between -15 and -1°C according to field measurements (Girard et al., 2013; Amitrano et al., 2012), numerical models (Walder and Hallet, 1985) and laboratory tests (Draebing and Krautblatter, 2019). My data showed the occurrence of cryogenic induced opening and closing at several crackmeters (Fig. 7b-d, 7h). The slow opening in combination with the temperature regime suggests that ice segregation is the driving process behind the observed crack opening. This opening can progressively weaken rockwall strength and potentially triggers rock slope failure as observed at Piz Kesch in winter 2014 (Phillips et al., 2016b). The length of the temperature window enabling ice segregation increases with altitude but is modulated by insulating snow cover. Climate change will shorten the snow duration by an earlier meltout date (Bender et al., 2020) and increase air and ground temperatures (Bender et al., 2020; Gobiet et al., 2014), therefore, the time period of temperature windows enabling ice segregation will decrease. This will affect especially rockwalls located at lower elevations, therefore, cryogenic processes and triggered rockfall will be shifted to higher elevations. At higher-elevations, the climate-changed induced changes of the temperature regime will also affect permafrost rockwalls, decrease rockwall stability (Draebing et al., 2014; Krautblatter et al., 2013) and increase rockfall activity due to increased thawing (Ravanel et al., 2010; Ravanel and Deline, 2010) amplified by temperature extremes (Gruber et al., 2004b; Ravanel et al., 2017)."

Numerical models show that thermal induced stresses can influence entire rock slopes. Therefore, the observed rock creeping pattern can affect whole slopes in terms of deep-seated rock slope deformation, a process widely distributed in the Alps. "Plastic deformation of fractures contributes to the preparation of rockfalls (Gunzburger et al., 2005). Previous studies demonstrated that thermal-induced crack deformation causes irreversible displacement of rock blocks (Weber et al., 2017; Hasler et al., 2012). Gunzburger et al. (2005) and do Amaral Vargas et al. (2013) suggested that thermal changes can cause rock creep along shear planes. My data demonstrates that rock blocks creep with a direction depending on shear plane dipping. Dipping out of the rockwall results in creeping that increases fracture opening (RW1, Fig. 10d) and can trigger rockslide processes. In contrast, dipping into the rockwall causes fracture closing (RW3, RWS; Fig. 10e). My observed blocks will not be released as rockfall, however, the observed mechanism can trigger a wedge failure in more steeper and overhanging rockwalls that are more susceptible to rockfall (Matasci et al., 2017). Several studies indicated that thermal-induced stresses can affect rock slopes up to 100 m depth (Gischig et al., 2011b) and affect deep-seated gravitational slope deformations (Gischig et al., 2011a; Rouyet et al., 2017; Watson et al., 2004). Therefore, thermal changes can decrease rock slope stability with time (preparatory factor) and potentially cause landsliding (triggering factor)."

The reviewer doubts that this study is of interest to a wider readership and I can only disagree. This study quantifies rock and fracture kinematics and partially stresses. It links these stresses to climate and discusses potential effects of climate change that can change rockfall in mountainous areas in the future. I admit that the first version of the manuscript was tedious and hid the major findings, however, I think these findings are presented in a concise and improved way in the revised version. Furthermore, I think the findings are of wider interest. I quantified climatic drivers of rockfall, which explain rockfall occurrences in Alpine environments and can be quantified by rockfall data in future studies.